

Non-perturbative QCD effects in jets at hadron colliders

Mrinal Dasgupta

*School of Physics and Astronomy, University of Manchester
Oxford Road, Manchester M13 9PL, U.K.
E-mail: dasgupta@hep.man.ac.uk*

Lorenzo Magnea

*Dipartimento di Fisica Teorica, Università di Torino, and
INFN, Sezione di Torino, Via P. Giuria, I-10125 Torino, Italy
E-mail: magnea@to.infn.it*

Gavin P. Salam

*LPTHE, CNRS UMR 7589; Université Pierre et Marie Curie (Paris VI); Université
Denis Diderot (Paris VII), 75252 Paris Cedex 05, France
E-mail: salam@lpthe.jussieu.fr*

ABSTRACT: We discuss non-perturbative QCD contributions to jet observables, computing their dependence on the jet radius R , and on the colour and transverse momentum of the parton initiating the jet. We show, using analytic QCD models of power corrections as well as Monte Carlo simulations, that hadronisation corrections grow at small values of R , behaving as $1/R$, while underlying event contributions grow with the jet area as R^2 . We highlight the connection between hadronisation corrections to jets and those for event shapes in e^+e^- and DIS; we note the limited dependence of our results on the choice of jet algorithm; finally, we propose several measurements in the context of which to test or implement our predictions. The results presented here reinforce the motivation for the use of a range of R values, as well as a plurality of infrared-safe jet algorithms, in precision jet studies at hadron colliders.

KEYWORDS: QCD, Jets.

Contents

1. Introduction	1
2. Perturbative R dependence	4
3. An analytical estimate for hadronisation corrections	7
3.1 Dipoles involving the trigger jet and incoming partons	10
3.2 Dipole involving the trigger and recoil jets	11
3.3 Incoming dipole	11
3.4 Dipoles involving incoming partons and the recoil jet	12
3.5 Leading power correction	12
3.6 Mass distribution	14
4. Comparison with Monte Carlo results	14
5. Experimental considerations	20
5.1 Radius optimisation	20
5.2 Measurement of $\langle\delta p_t\rangle$	23
5.3 Inclusive jet spectrum	26
6. Conclusions	28

1. Introduction

Jets play a key role in many experimental studies at the Tevatron, and will continue to do so at the LHC. They are useful, for example, in top reconstruction and mass measurements, in searches for the Higgs boson and new physics signals, and of course they are instrumental for QCD studies, such as inclusive-jet measurements, which in turn are an important input for the determination of parton distribution functions.

Jets, however, are fundamentally ambiguous objects, reflecting the fact that the divergences of QCD perturbation theory make it impossible to define clusters of final state hadrons uniquely assigned to individual hard partons emitted at leading order. Most procedures to cluster measured hadrons into jets, *i.e.* jet algorithms, deal with this ambiguity by introducing a resolution parameter to define when exactly a jet with substructure should actually be resolved into two jets. For currently used hadron-collider jet algorithms the main parameter is generally a threshold on the allowed opening angle of the jet, and is called R or jet radius (defined on the azimuth-rapidity cylinder).

Given, on the experimental side, the increased precision required for present hadron collider studies, and the complex hadronic environment expected in LHC final states, and

given many years of theoretical advances in our understanding of QCD, it is both useful and possible to work towards a better quantitative understanding of how the choice of the jet algorithm and the specification of its parameters influence the clustering of QCD radiation, and our general understanding of the final state in hadron collisions.

One can consider three classes of QCD effects: perturbative radiation, hadronisation and the underlying event. It should be realised that there is no unique, fully consistent, gauge-invariant way to distinguish these three classes: rather, one must try to define perturbation theory, and the underlying factorisation scheme, precisely enough, in order to identify non-perturbative hadronisation corrections without double counting; underlying event corrections will, at some level, inevitably mix with hadronisation: one must argue that this mixing does not occur, or is parametrically controllable, at least at leading and next-to-leading power in the hard scale. In this respect, as we will see, the radius dependence is a very useful tool. With this premise, one would like to understand how each of these classes of contributions affects the momentum of a jet, as a function of the jet radius R , as a function of the centre-of-mass energy, and as a function of the properties of the parton that initiated the jet, such as its colour charge and its transverse momentum.

These issues can be studied through parton-shower Monte Carlo generators, taking advantage of their detailed and well tested non-perturbative modelling. It can, however, be difficult to extract simple analytical understanding from such models. An alternative approach is to carry out analytical calculations directly. Perturbatively, one may work with soft and collinear approximations for gluon emission, and perform a resummation. The tools for this task, in the intricate case of jet production in hadron-hadron collisions, have been available for a long time [1–3], and phenomenological studies of the effects of soft and collinear logarithms near threshold have been performed, both for inclusive jet cross sections [4, 5] and for jet shapes [6]. It is well understood that these resummations carry nontrivial information on the parametric size of non-perturbative corrections, as discussed in [7]. Furthermore, one can carry out non-perturbative studies using renormalon and related approaches [8–11]; these suggest that the dynamics of Monte Carlo models can in some cases be reduced, for sufficiently inclusive observables, to a single non-perturbative parameter, multiplied by analytically calculable coefficients. These models have had considerable success in the context of e^+e^- and DIS (for reviews, see [12, 13]); in contrast, for QCD final-state observables at hadron colliders, only a handful of results exist, notably for the jet energy-flow profile [6], the out-of-plane momentum for Z +jet production [14] and away-from-jet energy flow [15].

It is perhaps worth emphasising that the non-perturbative corrections we are discussing, especially at moderate p_t , have an impact that is comparable to that of higher-order perturbative effects, and may affect in a crucial way precision studies for many observables, even in the nominally asymptotic energy regime probed by the LHC. This is a familiar issue from QCD studies at LEP and HERA, especially those concerning event shapes. In the context of hadron collider phenomenology, non-perturbative radiation from hadronisation and underlying event is, for example, the main source of uncertainty in the determination of the jet energy scale. This plays a key role in precision studies, as was shown at Tevatron [16]: each percentage point of uncertainty in the jet energy scale translates, for

example, into a 1 GeV uncertainty in the top mass, and into a 10% uncertainty in the single-inclusive jet p_t distribution at $p_t \sim 500$ GeV. In general, the steep slope of jet distributions amplifies the effects of comparatively small energy shifts due to non-perturbative radiation, and propagates their impact all the way to the highest energies [17]: this effect will actually be magnified at LHC, where the underlying event is expected to provide an energy density much higher than that measured at Tevatron.

In this paper, we begin to address quantitatively a number of issues related to non-perturbative corrections to jet observables at hadron colliders. We focus mostly on the radius dependence of non-perturbative effects, but examine also the dependence on the quantum numbers of the partons initiating the jets, and the effects of the choice of jet algorithm, thus complementing and extending the more qualitative statements found for example in [18, 19]. For the sake of completeness, and in order to be able to compare perturbative and non-perturbative effects as precisely as possible, we begin in Section 2 by reviewing and organising perturbative results at NLO. Similar results have been derived and used before in order, for example, to allow for a precise matching between resummed and NLO jet cross sections [5]. In Section 3, we move to the main subject of our analysis, and provide an analytical estimate for the change δp_t in the transverse momentum of a jet due to hadronisation, at leading power in p_t . We employ the techniques of the dispersive approach to power corrections, adapted to the environment of hadron collisions. Our main result concerns the radius dependence of δp_t , which behaves like $1/R$ at small R , in sharp contrast to the behaviour of underlying event contributions, which are expected to grow with the jet area and become negligible for very narrow jets. The $1/R$ dependence of δp_t could have been deduced from the analysis of [7], predicting a $1/(QR)$ correction to the jet cross section. This fact seems however not to have been widely appreciated. Relative to [7], here we work with fully-defined jet algorithms, we show that corrections of $\mathcal{O}(1)$ vanish, while those of $\mathcal{O}(R)$ have a small coefficient, we provide the relation between the coefficient of $1/R$ and the non-perturbative parameter α_0 used in event shape studies (cf. [13] and references therein), separately for quark- and gluon-induced jets, and we outline the class of jet algorithms for which this relation is expected to be exact.

In Section 4 we compare our analytical results with Monte Carlo simulations, while varying R , the main parameter entering the jet definition. We employ `Pythia` [20], as well as `Herwig` [21] (with `Jimmy` [22] providing the underlying event) to generate hadron level jet events, and we reconstruct the jets using different (IR safe) algorithms, for different parton channels and different centre of mass energies. It is possible to generate separately the hadronisation and underlying event components of δp_t with Monte Carlo simulations; the main result for the hadronisation contribution is a striking confirmation of our analytic expression: the four different jet algorithms that we employ all agree with each other and with the analytic result, both in shape and normalisation, within margins that are quite reasonable given the inherent approximations of both models. The underlying event component is certainly much less well understood; it is clear, in any case, that the momentum shift due to the underlying event grows with R , and for moderate values of R it is several times larger at LHC than at the Tevatron, as might be expected.

We conclude, in Section 5, by outlining some experimental consequences of our results

and discussing some possible measurements that could validate them. Specifically, we discuss the optimal choice of the jet radius R in different experimental circumstances, a practical way to measure the p_t shift due to hadronisation and underlying event, and the effect of such a shift on the single-inclusive jet p_t distribution.

We regard these results as a first step towards a detailed analysis of jet physics beyond fixed order perturbation theory, which could be improved upon in several ways: our analytic estimate could for example be made more precise by matching it to a resummed prediction for a specific jet distribution; in general, we expect that beyond the leading $1/R$ behaviour non-perturbative radiation will not simply shift the cross section but also change its shape, as seen for example in [15]. One also expects that the shift will not be universal across different observables and algorithms, since typical jet algorithms introduce nonlinearities that are likely to spoil the simple pattern of exponentiation that underlies the power of one-gluon results [23]: the effects of this breaking of universality could be studied both with analytical and Monte Carlo tools.

We believe, in any case, that our results strongly suggest that experimental collaborations should try to maximise the flexibility of their choices concerning jet analyses. A wealth of information, and perhaps even opportunities for discovery, can be missed, if future jet studies are confined to just one or two algorithms, and a handful of parameter sets, chosen ahead of time. LHC is a discovery machine, and in order to fully exploit its potential we must be prepared with a range of flexible tools, capable of meeting unexpected, as well as expected challenges.

2. Perturbative R dependence

We begin by reviewing the perturbative dependence on the jet radius R , for small values of R , where a priori one can expect a logarithmic enhancement originating from the collinear singularity that is approached when the jet becomes very narrow. Specifically, we observe that perturbative $\ln R$ terms (discussed on many occasions previously, [5, 24–27]) originate from the same phenomenon as the $1/R$ growth that we will find for hadronisation contributions: as the jet becomes narrow, partons radiated outside of it (in other words partons which are not recombined with the jet by the chosen jet algorithm) are allowed to become more and more collinear to the emitter, approaching the collinear-singular configuration. Since these contributions are uniquely associated with the outgoing jet, and are independent of the other hard emitters, they can be simply computed in the collinear approximation.

In order to perform explicit calculations, we need to pick specific observables. Let us first consider the loss of transverse momentum for a leading jet, which is of relevance for example when using the hardest pair of jets in an event to reconstruct the mass of a decayed massive particle. As an example, consider the quasi-collinear branching of a quark with transverse momentum p_t , which splits into a quark carrying a fraction z of the initial momentum, plus a gluon carrying the remaining fraction $1 - z$. Given that the probability of such a quasi-collinear branching is just the corresponding splitting function, one can easily write down an expression for the leading perturbative contribution, at small R , to

the average change in transverse momentum of a high p_t jet. One finds

$$\langle \delta p_t \rangle_{\text{pert}} = p_t \int \frac{d\theta^2}{\theta^2} \int dz (\max[z, 1-z] - 1) \frac{\alpha_s(\theta z(1-z)p_t)}{2\pi} P_{qq}(z) \Theta(\theta - f_{\text{alg}}(z)R). \quad (2.1)$$

Here we constructed the change in transverse momentum as the difference between the p_t of the leading jet (which can be a quark or a gluon jet, depending on whether z or $1-z$ is larger) and that of the initial quark, accounting for the splitting probability $P_{qq}(z)$, averaged over the essentially collinear branching. The Θ function constraint denotes the condition for non-recombination of the softer parton into the leading jet, and $f_{\text{alg}}(z)$ is a function that depends on the jet algorithm. In the k_t [28,29] and Cambridge/Aachen [30] algorithms (for detailed definitions, see section 4), for example, one merely requires that the small angle θ between the quark and gluon be greater than R , so that $f_{k_t}(z) = f_{\text{Cam}}(z) = 1$. For stable-cone based algorithms, such as SISCone [31]¹, one is required, in order to enforce stability, to first construct the energy-weighted centroid of the quark-gluon system, $\vec{n}_j = z\hat{n}_q + (1-z)\hat{n}_g$, where $\hat{n}_{q,g}$ are unit vectors along the the quark and gluon directions. One must then ensure that the angle between \vec{n}_j and the softer parton be greater than R , which implies that the parton will not be recombined. Projecting, for example, the unit vector along the jet $\hat{n}_j = \vec{n}_j/|\vec{n}_j|$ onto the gluon direction, in the small-angle limit one finds

$$\theta_{jg} = z\theta_{qg}, \quad (2.2)$$

relating the opening angle between the gluon and jet directions, θ_{jg} , to the quark-gluon opening angle $\theta_{qg} = \theta$. Non-recombination, for the case where the gluon is the softer parton, so that $z > 1/2$, requires $\theta_{jg} > R$, which in turn gives

$$\theta_{qg} > \frac{R}{z} = R \left(1 + \frac{1-z}{z} \right); \quad (2.3)$$

if on the other hand the quark is softer ($z < 1/2$), the corresponding result is obtained by replacing z with $1-z$ in Eq. (2.3). This leads to

$$f_{\text{cone}}(z) = 1 + \min \left(\frac{z}{1-z}, \frac{1-z}{z} \right). \quad (2.4)$$

As a consequence, for cone algorithms, the θ integral in Eq. (2.1) is cut off at R/z ($R/(1-z)$) for $z > 1/2$ ($z < 1/2$). The z -dependence of the integration region does not affect the coefficient of $\ln R$, but gives an R -independent shift, computed below. Note that this result is independent of the overlap threshold in the split-merge stage of SISCone and similar algorithms.

Let us now return to Eq. (2.1). The logarithmic behaviour comes from the θ integral, which is cut off by the Θ function at small angle, while the upper limit is given by the large-angle hard partonic structure of the event, and does not affect the R dependence in the present approximation. For a quark-initiated jet, define then

$$L_q \equiv \int dz \min(z, 1-z) P_{qq}(z) = C_F \left(2 \ln 2 - \frac{3}{8} \right), \quad (2.5)$$

¹At this order the Midpoint algorithm [32] behaves in the same way, however it suffers from infrared unsafety at higher orders.

while for a gluon-initiated jet the corresponding quantity is

$$L_g \equiv \int dz \min(z, 1-z) \left(\frac{1}{2} P_{gg}(z) + n_f P_{qg} \right) = C_A \left(2 \ln 2 - \frac{43}{96} \right) + n_f T_R \frac{7}{48}, \quad (2.6)$$

where we have included a 1/2 factor for Bose symmetry in the gg channel, and $P_{ij}(z)$ are the real emission parts of the leading order DGLAP splitting kernels. It is easy to verify that, for a jet originated by a parton of type i , Eq. (2.1) yields

$$\frac{\langle \delta p_t \rangle_{\text{pert}}}{p_t} = \frac{\alpha_s}{\pi} L_i \ln R + \mathcal{O}(\alpha_s), \quad (2.7)$$

in a fixed-coupling approximation, with corrections which are non-singular as $R \rightarrow 0$. The main feature of Eq. (2.7) is the logarithmic dependence on the radius R , which may spoil the convergence of the perturbative result at small R . For a complete description of the perturbative result at the smallest R values, one might need to resum this logarithmic enhancement to all orders, an analysis which we postpone to future work.

For completeness, we also compute the R -independent shift in transverse momentum between the stable-cone-type and k_t (or Cambridge) algorithms. It is defined by

$$\frac{\langle \delta p_t^{\text{cone}} \rangle_{\text{pert}} - \langle \delta p_t^{k_t} \rangle_{\text{pert}}}{p_t} = \frac{\alpha_s}{\pi} K_i \quad (2.8)$$

where again i labels the parton species and we find

$$\begin{aligned} K_q &= \int dz \min(z, 1-z) \ln(f_{\text{cone}}(z)) P_{qq}(z) \\ &= \left(-\frac{15}{16} + \frac{9}{8} \ln 2 + \ln^2 2 \right) C_F \simeq 0.323 C_F, \end{aligned} \quad (2.9)$$

for quarks, while for gluons one has

$$\begin{aligned} K_g &= \int dz \min(z, 1-z) \ln(f_{\text{cone}}(z)) \left(\frac{1}{2} P_{gg}(z) + n_f P_{qg} \right) \\ &= \left(-\frac{1321}{1152} + \frac{133}{96} \ln 2 + \ln^2 2 \right) C_A + \left(\frac{241}{576} - \frac{25}{48} \ln 2 \right) n_f T_R \simeq 0.294 C_A + 0.057 n_f T_R. \end{aligned} \quad (2.10)$$

Numerically, one notes that the $K_i \sim 0.3 L_i$. This is the cause of the feature (originally observed in [29]) that, perturbatively, k_t and cone algorithms behave similarly when $\ln R_{k_t} \simeq 0.3 + \ln R_{\text{cone}}$, or equivalently $R_{k_t} \simeq 1.35 R_{\text{cone}}$.

A similar analysis can be carried out for other observables as well. One can for example consider the single-inclusive jet p_t distribution. Assuming a spectrum that falls off as $1/p_t^n$ at Born level, one finds at NLO a $\ln R$ correction (in this case multiplying the Born level distribution $\propto 1/p_t^n$) which is still of the form of (2.7), but with new coefficients $L_q(n)$ and $L_g(n)$. Defining as usual

$$\psi(n) = \frac{d}{dn} \ln \Gamma(n) = -\gamma_E + \sum_{p=1}^{n-1} \frac{1}{p}, \quad (2.11)$$

one finds

$$\begin{aligned}
L_q(n) &= \int_0^1 dz (z^{n-1} + (1-z)^{n-1} - 1) P_{qq}(z) \\
&= -C_F \left(2\psi(n-1) + 2\gamma_E + \left(\frac{3}{n} - \frac{3}{2} \right) \right), \tag{2.12}
\end{aligned}$$

as well as

$$\begin{aligned}
L_g(n) &= \int dz (z^{n-1} + (1-z)^{n-1} - 1) \left(\frac{1}{2} P_{gg}(z) + n_f P_{qg} \right) \\
&= -C_A \left(2\psi(n-1) + 2\gamma_E + \frac{4}{n} - \frac{2}{n+1} + \frac{2}{n+2} - \frac{11}{6} \right) \\
&\quad + 2n_f T_R \left(\frac{2}{n+2} - \frac{2}{n+1} + \frac{1}{n} - \frac{1}{3} \right). \tag{2.13}
\end{aligned}$$

This pattern is general: for a generic jet observable, the logarithmic behaviour in R is dictated by collinear dynamics, and can be computed at NLO (and beyond) using only splitting function information rather than the full squared matrix element. In this regard, we note that Ref. [19] has discussed the R dependence of the average squared jet mass, observing that to first order in α_s it behaves as $\alpha_s R^2 p_t^2$.

3. An analytical estimate for hadronisation corrections

To be concrete, let us choose a definite process and observable. We consider single-inclusive jet production near partonic threshold in hadronic collisions, a process of current interest at the Tevatron and soon at the LHC. Our definition of threshold is that the scaled transverse momentum $x_t = 2p_t/\sqrt{s}$ approaches its kinematical limit $x_t = 1$, so that all the available collision energy is converted into the jet transverse momentum. We have in mind the rapidity-integrated distribution, which however is known to be well approximated near threshold by the value of the distribution at vanishing rapidity [5]. We work then in the partonic centre-of-mass frame, and place the trigger jet at vanishing rapidity, with no loss of generality. At Born level we have the kinematics

$$\begin{aligned}
p_1 &= \frac{\sqrt{s}}{2}(1, 0, 0, 1) \\
p_2 &= \frac{\sqrt{s}}{2}(1, 0, 0, -1) \\
p_3 &= p_j = p_t(1, 1, 0, 0) \\
p_4 &= p_r = p_t(1, -1, 0, 0)
\end{aligned} \tag{3.1}$$

where p_j is the four-momentum of the trigger jet, p_t its transverse momentum and p_r the four-momentum of the recoil jet. At Born level both jets correspond to massless particles and it follows that

$$p_t = \frac{\sqrt{s}}{2}. \tag{3.2}$$

Consider now the change in p_t induced by a soft gluon emission. We must separately consider two alternative scenarios: either the soft emission is recombined by the jet algorithm with the hard parton associated with the trigger jet, or it is left unrecombined, so that the measured jet remains massless at this order. The recombination scheme we choose is the one commonly used for jet studies at the Tevatron, the E scheme, where the four-momentum of the jet is obtained by adding the four-momenta of the constituent partons.

In the case where recombination happens the final state kinematics becomes

$$\begin{aligned} p_j &= (\sqrt{p_t^2 + M_j^2}, p_t, 0, 0) \\ p_r &= (p_t, -p_t, 0, 0) , \end{aligned} \quad (3.3)$$

where the trigger jet now has a mass M_j^2 , while the recoil jet is still a massless hard parton. Using energy conservation one has then

$$p_t + \sqrt{p_t^2 + M_j^2} = \sqrt{s} . \quad (3.4)$$

Expanding to first order in the mass M_j^2 (since the gluon we recombine with the jet has been assumed to be soft) we obtain

$$p_t = \frac{\sqrt{s}}{2} \left(1 - \frac{M_j^2}{s} \right) . \quad (3.5)$$

The change in p_t from its Born value is given by

$$\delta p_t^+(k) = -\frac{M_j^2}{2\sqrt{s}} = -\frac{p_3 \cdot k}{\sqrt{s}} , \quad (3.6)$$

where the + superfix denotes the case when the gluon is recombined with the jet, and we wrote the jet mass as $M_j^2 = (p_3 + k)^2 = 2p_3 \cdot k$, with p_3 the four-momentum of the hard massless parton initiating the jet, and k that of the soft gluon.

When the gluon is not recombined, the recoil system is massive and one similarly finds

$$\delta p_t^-(k) = -\frac{M_r^2}{2\sqrt{s}} = -\frac{p_4 \cdot k}{\sqrt{s}} , \quad (3.7)$$

where p_4 denotes the four-momentum of the massless hard parton recoiling against the trigger jet. Parametrising the soft gluon four-momentum as

$$k^\mu = k_t (\cosh \eta, \cos \phi, \sin \phi, \sinh \eta) , \quad (3.8)$$

where k_t , η and ϕ are respectively the transverse momentum, rapidity and azimuth defined with respect to the beam direction, it is easy to see that to first order in the small quantity k_t one has

$$\delta p_t^\pm(k) = -\frac{k_t}{2} (\cosh \eta \mp \cos \phi) . \quad (3.9)$$

To obtain the average change in jet p_t due to soft emissions, one has to multiply the result in Eq. (3.9), for the change in p_t due to a soft emission, times the probability of emitting

the soft gluon, and subsequently integrate over phase space. In the eikonal approximation, appropriate to soft emissions, the probability (squared matrix element) for the emission of a gluon with momentum k from an ensemble of hard partons with momenta p_i may be expressed as a sum over contributions from all possible colour dipoles

$$|\mathcal{M}|^2 = |\mathcal{M}_0|^2 \sum_{(ij)} C_{ij} W_{ij}(k) , \quad (3.10)$$

where the sum runs over all distinct pairs (ij) of hard partons, or equivalently, as stated before, over all dipoles. The quantity $|\mathcal{M}_0|^2$ is the squared matrix element for the hard scattering, which in our case has to be computed for each separate partonic subprocess contributing to the jet distribution, and contains the dependence on parton distribution functions. The contribution of each dipole W_{ij} is weighted by the colour factor $C_{ij} = -2(\mathbf{T}_i \cdot \mathbf{T}_j)$, where $\mathbf{T}_{i,j}$ are generators of SU(3) corresponding to the colour charges of partons i and j , while the kinematic factor $W_{ij}(k)$ is explicitly given by the classical antenna function

$$W_{ij}(k) = \frac{\alpha_s(\kappa_{t,ij})}{2\pi} \frac{p_i \cdot p_j}{(p_i \cdot k)(p_j \cdot k)} \quad (3.11)$$

where α_s is defined in the bremsstrahlung scheme [33], and its argument is the invariant quantity $\kappa_{t,ij}^2 = 2(p_i \cdot k)(p_j \cdot k)/(p_i \cdot p_j)$, which is just the transverse momentum with respect to the dipole axis, in the dipole rest frame. Assembling these results one can write an expression for the average shift in the jet transverse momentum when a soft gluon is emitted in a selected partonic channel. These shifts must then be recombined with the proper weights when the full cross section is built by summing over the various hard scattering processes contributing to a given distribution. In any selected channel we write

$$\langle \delta p_t \rangle = \sum_{(ij)} C_{ij} \int dk_t k_t d\eta \frac{d\phi}{2\pi} \frac{\alpha_s(\kappa_{t,ij})}{2\pi} \frac{(p_i \cdot p_j)}{(p_i \cdot k)(p_j \cdot k)} \delta p_t(k) , \quad (3.12)$$

where we integrated over the soft gluon phase space and we defined

$$\delta p_t(k) = \delta p_t^+(k) \Theta_{\text{in}} + \delta p_t^-(k) \Theta_{\text{out}} , \quad (3.13)$$

with Θ_{in} being unity if the gluon is inside the jet and zero otherwise, and conversely for Θ_{out} . To extract the part of the soft contribution that one can associate with non-perturbative hadronisation effects, $\langle \delta p_t \rangle_{\text{h}}$, one simply considers the region $\kappa_{t,ij} < \mu_I$ in Eq. (3.12), with μ_I an infrared factorisation scale, to be chosen so that above μ_I one may safely use perturbation theory. The coupling α_s , which is perturbatively divergent in this region, is now to be replaced by a universal, non-perturbatively defined, finite quantity, whose moments at low energy are expected to be observable. In addition, one has to remove the contribution to Eq. (3.12) that would be included in fixed-order perturbative contributions, so that one is left with a pure hadronisation piece, which can subsequently be combined with fixed order perturbation theory without double counting. In Eq. (3.12) we replace then the coupling $\alpha_s(\kappa_t)$ with $\delta\alpha_s(\kappa_t) = \alpha_s(\kappa_t) - \alpha_s^{\text{PT}}(\kappa_t)$, where $\alpha_s^{\text{PT}}(\kappa_t)$ is the standard perturbative coupling, which can be expanded in powers of $\alpha_s(p_t)$ to the desired

order of perturbation theory. We note that the standard choice for μ_I in the case of LEP event-shape studies was 2 GeV, but it should be emphasised that the sensitivity to the choice of this scale is only $\mathcal{O}(\alpha_s^{n+1})$, if one correctly combines the non-perturbative result with perturbative corrections evaluated to $\mathcal{O}(\alpha_s^n)$ [13].

Let us continue by writing, purely for the sake of calculational convenience,

$$\delta p_t(k) = \delta p_t^-(k) + (\delta p_t^+(k) - \delta p_t^-(k)) \Theta_{\text{in}} , \quad (3.14)$$

where we used the fact that $\Theta_{\text{out}} + \Theta_{\text{in}} = 1$. In this way, we have divided the integral in Eq. (3.12) into a ‘global’ term, involving an integral over all of phase space of the unrecombined gluon contribution δp_t^- , and a term involving an integral over the interior of the jet region. We demonstrate in the Appendix that the global term does not produce a leading power correction, so that the complete leading contribution arises from the term involving the integral over the jet region.

We note here that at the level of the single-gluon calculation all the jet algorithms function in an identical manner, so that a soft gluon is recombined with a hard parton (and $\Theta_{\text{in}} = 1$) if $\delta\eta^2 + \delta\phi^2 < R^2$. In the present case, since we have fixed the trigger jet at $\eta = \phi = 0$, the gluon is in the jet for $\eta^2 + \phi^2 < R^2$. As noted above, the only relevant contribution to the present accuracy arises from the second term in the sum on the RHS of Eq. (3.14). As a consequence, we only need to evaluate integrals of the form

$$\langle \delta p_t \rangle_{\text{h}} = \sum_{i,j} C_{ij} \int dk_t k_t d\eta \frac{d\phi}{2\pi} \frac{\delta\alpha_s(\kappa_{t,ij})}{2\pi} \frac{(p_i \cdot p_j)}{(p_i \cdot k)(p_j \cdot k)} (\delta p_t^+ - \delta p_t^-) \Theta_{\text{in}} \theta(\mu_I - \kappa_{t,ij}) , \quad (3.15)$$

for each dipole, recombined with the colour factors appropriate to the parton channel being considered.

3.1 Dipoles involving the trigger jet and incoming partons

Consider first the dipole formed by one of the incoming partons (say the one with four momentum p_1) and the outgoing hard parton corresponding to the trigger jet, which we denote with the label $(1j)$. The transverse momentum with respect to this dipole is given by

$$\kappa_{t,1j}^2 = 2 \frac{(p_1 \cdot k)(p_j \cdot k)}{(p_1 \cdot p_j)} = 2 k_t^2 (\cosh \eta - \cos \phi) . \quad (3.16)$$

Using $\delta p_t^+(k) - \delta p_t^-(k) = k_t \cos \phi$, and changing variables from k_t to $\kappa_{t,1j}$ (since the factorisation scale μ_I sets a limit on the range of $\kappa_{t,1j}$, not of k_t), we obtain

$$\langle \delta p_t \rangle_{\text{h}}^{(1j)} = C_{1j} \frac{1}{2} \mathcal{A}(\mu_I) \int_{\eta^2 + \phi^2 < R^2} d\eta \frac{d\phi}{2\pi} e^{3\eta/2} \frac{\cos \phi}{\sqrt{2} (\cosh \eta - \cos \phi)^{\frac{3}{2}}} , \quad (3.17)$$

where we defined the first moment of the non-perturbative coupling $\delta\alpha_s$ below the factorisation scale as

$$\mathcal{A}(\mu_I) = \frac{1}{\pi} \int_0^{\mu_I} d\kappa_t \delta\alpha_s(\kappa_t) . \quad (3.18)$$

In order to make an explicit connection with event shape studies [13], we can rewrite Eq. (3.18) in more detail as

$$\mathcal{A}(\mu_I) = \frac{1}{\pi} \mu_I \left[\alpha_0(\mu_I) - \alpha_s(p_t) - \frac{\beta_0}{2\pi} \left(\ln \frac{p_t}{\mu_I} + \frac{K}{\beta_0} + 1 \right) \alpha_s^2(p_t) \right], \quad (3.19)$$

where $\alpha_0 \equiv (1/\mu_I) \int_0^{\mu_I} \alpha_s(k_t) dk_t$ is the average coupling over the infrared region, familiar from event shape studies, and we have carried out the subtraction of the perturbative coupling, $\alpha_s(p_t)$, to two-loop accuracy in the $\overline{\text{MS}}$ scheme, where $K = C_A \left(\frac{67}{18} - \frac{\pi^2}{6} \right) - \frac{5}{9} n_f$. Note that similar expressions in Ref. [13] are rescaled by the Milan factor, accounting for gluon decays; this rescaling will be discussed below, in Section 3.5.

The integral over the soft gluon direction can be evaluated by choosing polar coordinates in the $\eta - \phi$ plane and expanding in powers of the radial variable. Discarding the spurious collinear divergence arising when the gluon is emitted along the outgoing leg, which cancels against an identical one in the ‘global’ term, as shown in the Appendix, one finds

$$\langle \delta p_t \rangle_h^{(1j)} = C_{1j} \mathcal{A}(\mu_I) \left(-\frac{1}{R} + \frac{5}{16} R - \frac{23}{3072} R^3 - \frac{95}{147456} R^5 + \mathcal{O}(R^7) \right). \quad (3.20)$$

By symmetry, an identical result is obtained for the $2j$ dipole, formed by the trigger hard parton and the other incoming parton with momentum p_2 .

3.2 Dipole involving the trigger and recoil jets

In this case the transverse momentum of the soft gluon with respect to the dipole, which we label with (jr) , is given by

$$\kappa_{t,jr}^2 = k_t^2 e^{-\eta} (\cosh^2 \eta - \cos^2 \phi), \quad (3.21)$$

which leads to the integral

$$\langle \delta p_t \rangle_h^{(jr)} = C_{jr} \mathcal{A}(\mu_I) \int_{\eta^2 + \phi^2 < R^2} d\eta \frac{d\phi}{2\pi} \frac{\cos \phi}{(\cosh^2 \eta - \cos^2 \phi)^{3/2}}. \quad (3.22)$$

This can be evaluated as before, using polar coordinates and expanding in powers of R . One finds

$$\langle \delta p_t \rangle_h^{(jr)} = C_{jr} \mathcal{A}(\mu_I) \left(-\frac{1}{R} - \frac{1}{4} R + \frac{1}{192} R^3 - \frac{5}{2304} R^5 + \mathcal{O}(R^7) \right). \quad (3.23)$$

3.3 Incoming dipole

The dipole involving the two incoming partons, labelled as (12), is the simplest to compute, since in this case $\kappa_{t,12} = k_t$. For this dipole the integration over the interior of the jet does not produce a $1/R$ correction, since there is no collinear enhancement for radiation emitted by the incoming partons as the jet becomes narrow. We expect radiation from this dipole

to behave essentially like an underlying event contribution, and this is in fact what we find. The relevant integral is

$$\begin{aligned}
\langle \delta p_t \rangle_{\text{h}}^{(12)} &= C_{12} \mathcal{A}(\mu_I) \int_{\eta^2 + \phi^2 < R^2} d\eta \frac{d\phi}{2\pi} \cos \phi \\
&= C_{12} \mathcal{A}(\mu_I) R J_1(R) \\
&= C_{12} \mathcal{A}(\mu_I) \left(\frac{1}{2} R^2 - \frac{1}{16} R^4 + \frac{1}{384} R^6 + \mathcal{O}(R^8) \right), \tag{3.24}
\end{aligned}$$

where J_1 is the Bessel function of the first kind.

3.4 Dipoles involving incoming partons and the recoil jet

As these dipoles involve radiation which is not associated with the trigger jet, we expect, and verify, that they do not generate any $1/R$ enhancement. Considering for example the $(1r)$ dipole, the relevant transverse momentum is

$$\kappa_{t,1r}^2 = 2 k_t^2 e^{-\eta} (\cosh \eta + \cos \phi), \tag{3.25}$$

which leads to the integral

$$\langle \delta p_t \rangle_{\text{h}}^{(1r)} = C_{1r} \frac{1}{2} \mathcal{A}(\mu_I) \int_{\eta^2 + \phi^2 < R^2} d\eta \frac{d\phi}{2\pi} \frac{e^{\frac{3\eta}{2}} \cos \phi}{\sqrt{2} (\cosh \eta + \cos \phi)^{\frac{3}{2}}}. \tag{3.26}$$

This gives

$$\langle \delta p_t \rangle_{\text{h}}^{1r} = C_{1r} \mathcal{A}(\mu_I) \left(\frac{1}{16} R^2 + \frac{5}{512} R^4 - \frac{95}{49152} R^6 + \mathcal{O}(R^8) \right). \tag{3.27}$$

Clearly, the $(2r)$ dipole gives an identical contribution.

3.5 Leading power correction

Having computed the results for each individual dipole, we can now perform the sum in Eq. (3.10) to obtain our estimate for the shift in the jet p_t due to hadronisation effects. We concentrate on the leading behaviour at small R , including terms up to $\mathcal{O}(R)$, since at large values of R we expect the hadronisation component to be dominated by the underlying event contribution, which behaves like R^2 . Clearly, each parton channel will have a different p_t shift, because of the different colour weights in Eq. (3.10). Here we choose as an example, to illustrate our point, the scattering of non-identical quarks,

$$q(p_1) + q'(p_2) \rightarrow q(p_3) + q'(p_4). \tag{3.28}$$

The calculation of the colour weight of the various dipoles in Eq. (3.10) is a textbook exercise [34]. The result is

$$\left| \mathcal{M}^{qq' \rightarrow qq'g} \right|^2 = \left| \mathcal{M}_0^{qq' \rightarrow qq'} \right|^2 \left(2C_F (W_{14} + W_{23}) + \frac{1}{N_c} [W_{12}; W_{34}] \right), \tag{3.29}$$

where, in a notation similar to [34], we have defined

$$[W_{12}; W_{34}] = 2W_{12} + 2W_{34} - W_{13} - W_{14} - W_{23} - W_{24} , \quad (3.30)$$

which is a collinear finite combination of dipoles contributing at subleading order in the number of colours N_c . Since we are interested in just the $1/R$ and R terms, we need only consider dipoles that involve the hard parton responsible for the trigger jet, which we identify with the quark carrying momentum p_3 . Adding together the contributions from the relevant dipoles one easily finds

$$\langle \delta p_t \rangle_h^{qq' \rightarrow qq'} = \mathcal{A}(\mu_I) \left[-\frac{2}{R} C_F + \frac{1}{8} R \left(5C_F - \frac{9}{N_c} \right) + \mathcal{O}(R^2) \right] . \quad (3.31)$$

We note several features of Eq. (3.31), most of which are common to the other parton channels as well. The most striking aspect is clearly the singular dependence on the jet radius R , arising from all dipoles involving the trigger jet. This singular behaviour is a reflection of the fact that, as one makes the jet narrower, one increases the p_t loss due to hadronisation, which also explains the negative sign of the leading term. The leading behaviour as $R \rightarrow 0$ arises from the collinear singularity of the matrix element, which is also responsible for the $\ln R$ enhancement of the perturbative result described in Sect. 2. For this reason, one expects the $1/R$ behaviour to be accompanied by the colour charge of the parton initiating the jet, which in the above case is C_F , and this expectation is indeed confirmed when one combines the dipoles. When the trigger jet originates from a gluon, as it would be for instance in the $gg \rightarrow gg$ channel, the leading $1/R$ behaviour of the hadronisation correction can thus be simply obtained with the replacement $C_F \rightarrow C_A$.

Another point to note about the $1/R$ term in Eq. (3.31) is the fact that its coefficient, $2C_F \mathcal{A}(\mu_I)$, is one half of the coefficient of the $1/Q$ correction to the thrust variable in e^+e^- annihilation, as computed in [8]. In order to match more recent evaluations [35–39], this result for the thrust must actually be rescaled by a factor $\frac{2}{\pi} M$, where M is the Milan factor. Specifically, the factor $\frac{2}{\pi}$ accounts for the use of a fully dispersive coupling (one expressed in terms of the gluon virtuality rather than its transverse momentum), while the Milan factor M accounts for the non-inclusiveness of final-state observables, *i.e.* the fact that a virtual gluon inevitably splits into massless objects, but the observable may change its value unless all of the gluon decay products are emitted into the appropriate region of phase space. For observables that are linear in multiple soft-gluon momenta, the Milan factor is independent of all other details of the observable, and numerically one finds $M \simeq 1.49$ (for $n_f = 3$ in the non-perturbative region), or equivalently $\frac{2}{\pi} M \simeq 0.95$, which is a modest overall correction. We note, however, that jet transverse momenta are in general *not* linear in soft-gluon momenta, because of the non-trivial way in which soft-particles recombine with each other and into jets. The one known exception in this respect, among infrared and collinear safe jet algorithms, is the anti- k_t algorithm², introduced and discussed at length in [40]. Thus, while at present we can tentatively associate the size of our $1/R$ effect with the thrust calculation, this implicitly assumes that an analysis similar

²More generally, all algorithms with $p < 0$ in Eq. (4.5).

to that performed in Refs. [35, 36, 38] will yield results that do not differ significantly from the value computed for M in the case of linear observables.

We finally observe that the coefficient of the term linear in R in Eq. (3.31) is numerically less than 20% of the coefficient of the $1/R$ term. This means that the $1/R$ behaviour should be a good approximation to the full result over a wide range of values of R , up to $R \sim 1$, a fact which will be useful to construct simple approximate formulae in Section 5.

3.6 Mass distribution

In order to illustrate the generality of the method, let us briefly summarise the results one obtains when performing the same computation with a different observable. We now compute the hadronisation correction to the jet mass, δM_j^2 , using the framework described above. Working again near threshold, the variation in the jet mass due to the emission of a single soft gluon is given by

$$\delta M_j^2(k_t, \eta, \phi) = 2p_j \cdot k = k_t \sqrt{s} (\cosh \eta - \cos \phi) , \quad (3.32)$$

provided the jet algorithm recombines the gluon with the jet. Clearly, there is no correction if the gluon is not recombined. As the singular $1/R$ behaviour of the hadronisation correction to the transverse momentum of the jet was due to *unrecombined* gluons becoming increasingly collinear to the originating hard parton when $R \rightarrow 0$, there should be no corresponding singular piece for the jet mass. We find in fact that the leading power corrections vanish at least as R for all dipoles. Specifically

$$\begin{aligned} \delta M_{j,12}^2 &= C_{12} \mathcal{A}(\mu_I) \frac{\sqrt{s}}{2} \left(\frac{1}{4} R^4 + \frac{1}{4608} R^8 + \mathcal{O}(R^{12}) \right) , \\ \delta M_{j,1j}^2 &= C_{1j} \mathcal{A}(\mu_I) \frac{\sqrt{s}}{2} \left(R + \frac{3}{16} R^3 + \frac{125}{9216} R^5 + \frac{7}{16384} R^7 + \mathcal{O}(R^9) \right) , \\ \delta M_{j,jr}^2 &= C_{jr} \mathcal{A}(\mu_I) \frac{\sqrt{s}}{2} \left(R + \frac{5}{576} R^5 + \mathcal{O}(R^9) \right) , \\ \delta M_{j,1r}^2 &= C_{1r} \mathcal{A}(\mu_I) \frac{\sqrt{s}}{2} \left(\frac{1}{32} R^4 + \frac{3}{256} R^6 + \frac{169}{589824} R^8 + \mathcal{O}(R^{10}) \right) . \end{aligned} \quad (3.33)$$

We observe that the small radius behaviour of the leading power correction to the jet mass distribution is softened with respect to the p_t distribution by two powers of R . This is a consequence of the fact that gluons emitted inside small cones make small contributions to the jet mass, just as for the p_t distribution. Gluons which are not recombined with the jet, on the other hand, in this case make no contribution, so that the singular behaviour at small R is absent. Note however that the contribution of the underlying event to the jet mass is $\mathcal{O}(R^4)$, so that again the hadronisation component dominates by three powers of R , for $R < 1$.

4. Comparison with Monte Carlo results

Two simple results emerge from the analytic approach of Section 3, concerning our expectations for the non-perturbative modification of a jet transverse momentum. First,

non-perturbative radiation associated with emission from the jet’s originating parton, in a selected production channel, should modify the jet p_t as

$$\langle \delta p_t \rangle_h = -C_i \frac{2}{R} \mathcal{A}(\mu_I) + \mathcal{O}(R) , \quad (4.1)$$

where C_i is the colour charge appropriate to the parton originating the jet³. Recall that, in the single soft gluon approximation the scale $\mathcal{A}(\mu_I)$ is related to the scale appearing in analytical studies of hadronisation in e^+e^- and DIS collisions. A first test of our approach would then be to fit data for jet distributions using expressions like Eq. (4.1), with a numerical value for $\mathcal{A}(\mu_I)$ borrowed from event shape studies, including the appropriate Milan factor, as discussed in Sect. 3.5. We must then expect some degree of loss of universality across different algorithms and observables, which introduce different nonlinear multi-gluon effects. For our illustrative purposes, however, it is sufficient to be aware that $2C_F \mathcal{A}(2\text{GeV}) \simeq 0.5 \text{ GeV}$, corresponding to the amount of non-perturbative transverse momentum radiated per unit rapidity with respect to a $q\bar{q}$ dipole, while a gg dipole must be reweighted by a factor $C_A/C_F = 9/4$.

Our second result is that corrections associated with the dipole of incoming partons, and in fact more generally with any dipole not involving the trigger jet, give a contribution that scales as R^2 , *i.e.* in proportion to the jet area. These corrections effectively mimic underlying event corrections, and are indistinguishable from them. Borrowing our result in Sect. 3.3, and denoting the scale of transverse momentum emission per unit rapidity along the beam direction with Λ_{UE} , we expect the jet transverse momentum to be modified as⁴

$$\langle \delta p_t \rangle_{UE} = \Lambda_{UE} R J_1(R) = \frac{\Lambda_{UE}}{2} (R^2 - R^4/8 + \mathcal{O}(R^6)) . \quad (4.2)$$

The scale Λ_{UE} , as the notation suggests, cannot be easily related to $\mathcal{A}(\mu_I)$, since it receives contributions from the underlying event, *i.e.* the interactions between the proton remnants. The functional dependence on R through the combination $RJ_1(R)$ corresponds to the definition of ‘passive vector area’ of a jet given in Ref. [41, 42].

It is of interest to compare the two sets of contributions, Eq. (4.1) and Eq. (4.2), to what is observed in parton-shower Monte Carlo event generators. To do so, we begin by generating dijet events; after parton showering, we identify jets with a chosen jet algorithm, and label the transverse momenta of the two hardest jets as $p_{t,\text{ps}}^{(i)}$, ($i = 1, 2$); we select events for which the hardest jet satisfies $55 \text{ GeV} < p_{t,\text{ps}}^{(1)} < 70 \text{ GeV}$; next, we allow either the hadronization stage to take place, or both hadronization and underlying event generation; finally, we rerun the jet finder. After hadronization the two jet transverse momenta will be changed, and we denote them with $p_{t,\text{h}}^{(i)}$; similarly, after generating also the underlying

³As noted in the Introduction, this form of R dependence for the leading power correction was already suggested in [7] and its full form could probably have been deduced from [6]. It seems, however, from discussions of hadronisation in the literature [17, 18], that the community was not aware of the implications of these results.

⁴The terms of higher order in R are specific to our chosen recombination scheme, the E -scheme or four-vector recombination.

event, the momenta will become $p_{t,\text{UE}}^{(i)}$. At this point, we can define the hadronization contribution to the jet transverse momentum to be

$$\langle \delta p_t \rangle_{\text{h}} = \frac{1}{2} \left\langle p_{t,\text{h}}^{(1)} - p_{t,\text{ps}}^{(1)} + p_{t,\text{h}}^{(2)} - p_{t,\text{ps}}^{(2)} \right\rangle, \quad (4.3)$$

while the underlying event contribution is

$$\langle \delta p_t \rangle_{\text{UE}} = \frac{1}{2} \left\langle p_{t,\text{UE}}^{(1)} - p_{t,\text{ps}}^{(1)} + p_{t,\text{UE}}^{(2)} - p_{t,\text{ps}}^{(2)} \right\rangle - \langle \delta p_t \rangle_{\text{h}}. \quad (4.4)$$

Note that with most modern underlying event (UE) models it is not possible to carry out the UE generation independently from hadronization: one must first determine $\langle \delta p_t \rangle_{\text{h}}$ with the global UE switch turned off, and subsequently carry out a separate run with the switch turned on, in order to deduce $\langle \delta p_t \rangle_{\text{UE}}$.

Our results are shown in Fig. 1 for four different jet algorithms, as a function of the jet radius R , for $qq \rightarrow qq$ interactions (summing over the flavors and antiflavours of the incoming and outgoing quarks) in $p\bar{p}$ collisions, in Tevatron Run II kinematics, $\sqrt{s} = 1.96$ TeV. The upper curves in each plot are for $\langle \delta p_t \rangle_{\text{UE}}$, while the lower ones show $\langle \delta p_t \rangle_{\text{h}}$. In each case we show results from `Pythia` 6.4 [20], (tune A, using the default, ‘old’ shower), and from `Herwig` 6.5 [21] with the Jimmy UE model [22] (with the Atlas tune [43]). Additionally, for the hadronization results, we show the prediction based on the one-gluon emission approximation and universality assumption, Eq. (4.1).

The four jet algorithms we use are all infrared and collinear (IRC) safe, as they must be for any analysis beyond leading order. Specifically, three of the algorithms we use are sequential recombination algorithms; they operate by defining interparticle and beam-particle distance measures via

$$d_{ij}^{(p)} \equiv \min(k_{t,i}^{2p}, k_{t,j}^{2p}) \frac{\Delta y_{ij}^2 + \Delta \phi_{ij}^2}{R^2}, \quad d_{iB}^{(p)} \equiv k_{t,i}^{2p}, \quad (4.5)$$

and then recombining particles i and j if one of the $d_{ij}^{(p)}$ is smallest, or defining particle i as a jet, and removing it from the list of particles, if $d_{iB}^{(p)}$ is smallest; the procedure is then iterated until no particles are left. The choice $p = 1$ corresponds to the well-known (inclusive) k_t algorithm [28, 29]. Choosing $p = 0$ gives the Cambridge/Aachen algorithm [30], probably the simplest possible IRC-safe hadron-collider jet algorithm, corresponding to the successive recombination of particles that are closest on the $y - \phi$ cylinder, until all are separated by at least R . Its simplicity makes it our preferred choice in those figures where for brevity we consider only a single algorithm. Our third choice, $p = -1$, dubbed ‘anti- k_t ’ algorithm, is novel [40], and has several interesting properties: for example, it behaves like a perfect cone algorithm, in that hard jets are nearly always circular, with radius R on the $y - \phi$ cylinder; furthermore, it behaves linearly in soft gluon momenta, so that its hadronization corrections should have better universality properties, as was the case for event shapes in e^+e^- annihilation. As a fourth example, we use a seedless stable-cone algorithm, the SISCone algorithm [31], with a Tevatron run II type of split-merge procedure [32]. It is similar to the midpoint algorithm [32] used at Tevatron, differing mainly in its seedless nature and the resulting fact that it is IRC safe at all orders.

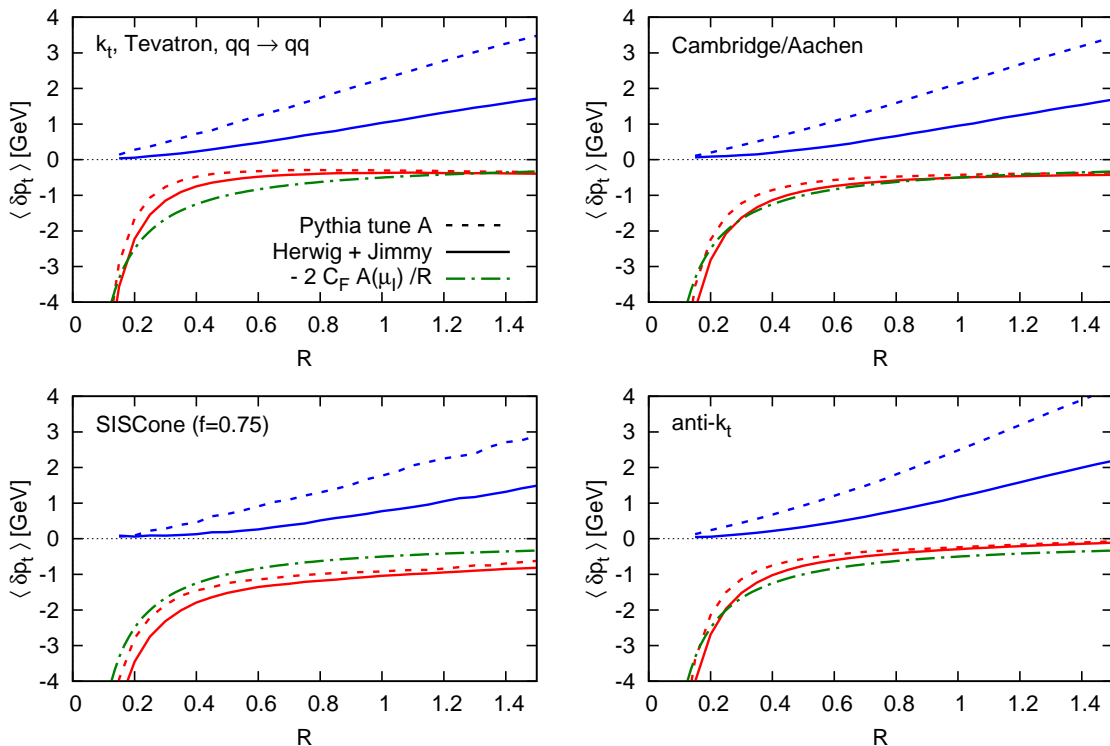


Figure 1: Modification of the p_t of jets due to the underlying event (upper curves) and hadronization (lower curves), for $qq \rightarrow qq$ scattering at the Tevatron Run II ($p\bar{p}$, $\sqrt{s} = 1.96$ TeV), comparing Pythia 6.412 [20] (tune A) and Herwig 6.510 [21] with Jimmy 4.3 [22]. In the case of hadronization the Monte Carlo outputs are compared to the analytical result, Eq. (4.1). Dijet events are selected containing an underlying $qq \rightarrow qq$ scattering, and with the requirement that at parton shower level the hardest jet has $55 \text{ GeV} < p_{t,\text{ps}} < 70 \text{ GeV}$. The non-perturbative corrections shown correspond to the average for the two hardest jets.

A striking feature of Fig. 1 is that all four jet algorithms have similar R dependences: despite much debate about the relative merits of different algorithms, they all behave identically in the presence of a single soft gluon, and, as a consequence, there are strong similarities in their non-perturbative behaviour.

The non-perturbative contribution that is generally acknowledged as being best modelled is hadronization: indeed the Monte Carlo models agree well between each other, as is natural given the extensive tuning of the hadronization-related parameters at LEP. The analytical prediction, Eq. (4.1), reproduces both the shape and normalisation relatively well, though the quality of agreement varies somewhat with the algorithm: the k_t (SISCone) algorithm, for example, has slightly less (more) negative corrections than predicted. These differences may be a reflection of the breakdown of the single gluon approximation, caused by non-linearity of the k_t , Cambridge/Aachen and SISCone algorithms. A full treatment would involve the inclusion in Eq. (4.1) of the non-trivial corrections associated with double-soft gluon emission, *i.e.* the (non-universal) Milan factor. Clearly, this would be of interest for further study.

The dependence of the hadronization contribution on the jet colour factor is visible

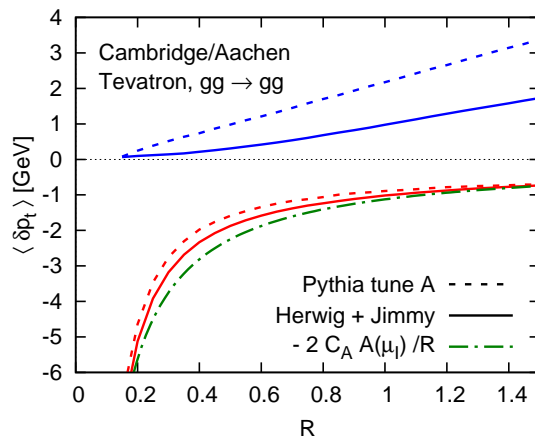


Figure 2: Similar to Fig. 1, but for the $gg \rightarrow gg$ underlying scattering channel, instead of $qq \rightarrow qq$. For brevity only the Cambridge/Aachen result is shown.

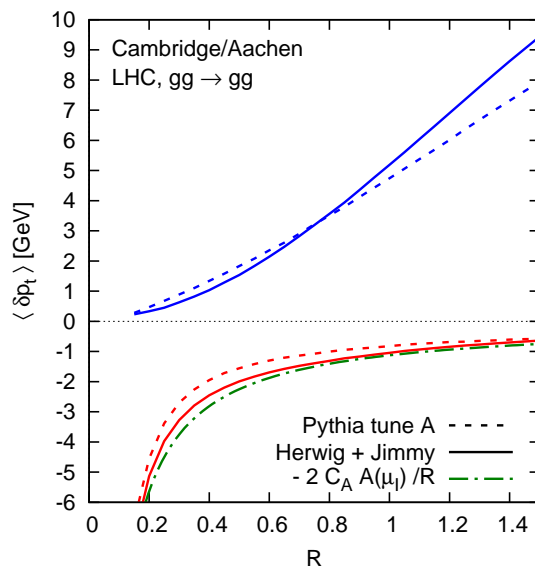


Figure 3: Similar to Fig. 2, but for the LHC (pp , $\sqrt{s} = 14$ TeV) rather than the Tevatron.

in Fig. 2, which displays results for the $gg \rightarrow gg$ channel at Tevatron. We see that the hadronization contribution roughly doubles compared to $qq \rightarrow qq$ scattering, again in reasonable agreement with the analytical prediction. Fig. 3, on the other hand, shows the independence of the hadronization contribution on collider energy, displaying results for $gg \rightarrow gg$ scattering at LHC, which are easily seen to be almost identical to the Tevatron results.

Underlying event contributions are much less well understood than hadronization. Not only is no analytical prediction available for their normalisation, but Pythia tune A and the Jimmy Atlas tune, despite both being tuned to similar Tevatron data, give underlying event correction to jet p_t 's that differ by a factor of two at the Tevatron, as is visible in Figs. 1 and 2. As can also be seen from these figures, the UE contribution is largely independent of the hard scattering channel ($qq \rightarrow qq$ versus $gg \rightarrow gg$). It does however

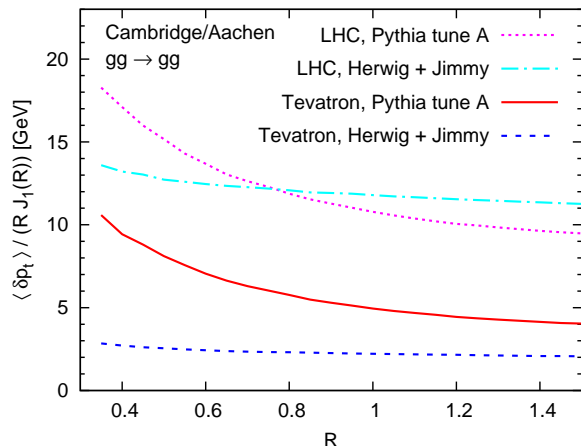


Figure 4: Plot of the UE contribution to the jet p_t , for Tevatron and LHC $gg \rightarrow gg$ events (selected as in Fig. 1), rescaled by the factor $RJ_1(R)$, corresponding to the passive area [41], as calculated for a 1-particle jet.

depend strongly on the collider energy, as seen in Fig. 3, which illustrates the huge size of the UE contribution predicted by Monte Carlo models at LHC. Interestingly, though *Jimmy* and *Pythia* differ for the Tevatron, they agree for LHC⁵.

Let us now turn to the functional form of the UE corrections, Eq. (4.2), and the interpretation of its normalisation. We consider $\langle \delta p_t \rangle_{\text{UE}}$ divided by its predicted R dependence, given by $RJ_1(R)$; this should give an R -independent result equal to Λ_{UE} . The results are shown in Fig. 4. Whereas for *Jimmy* there is near perfect agreement with the scaling prediction, with *Pythia* there is clear deviation from it towards small⁶ values of R , which can be interpreted as a correlation between underlying event activity and the properties of the hard scattering. Further investigation reveals that this is caused by strong colour reconnections in the *Pythia* underlying event model and tunes, an effect which is enhanced for $gg \rightarrow gg$ scattering as compared to $qq \rightarrow qq$ scattering⁷. Note in any case that the physical impact of this correlation is limited, since the relative deviation from the expected $RJ_1(R)$ form is significant only in the region where the absolute size of the UE contribution is modest.

Finally, let us comment on the physical scale associated with the underlying event, Λ_{UE} . At the Tevatron the value that emerges from the models is $\Lambda_{\text{UE}}(1.96 \text{ TeV}) \simeq 2 - 4 \text{ GeV}$, while at LHC it is $\Lambda_{\text{UE}}(14 \text{ TeV}) \simeq 10 \text{ GeV}$. This is an order of magnitude larger than the

⁵We have also examined other *Pythia* tunes (DW, DWT, S0, S0A). All are nearly identical at Tevatron energies, while, at LHC, tunes DW and S0A are similar to tune A, and tunes S0 and DWT give results that are about 40 – 50% higher.

⁶Note however that we are unable to consider the smallest R values, because the subtraction procedure in Eq. (4.4) makes it difficult to determine accurately the small UE contribution relative to the large hadronization effect.

⁷This feature is present to the same degree in tunes DW, DWT based on the old shower, and in all cases in which the old shower is used, it seems to be independent of the precise procedure used to extract the UE contribution. In tunes S0 and S0A, based on the new shower, it seems that the effect may be less strong, however it is difficult to make a firm statement because at small and moderate R the extraction of $\langle \delta p_t \rangle_{\text{UE}}$, eq. (4.4), is affected by non-trivial interplays between the parton shower and the UE multiple interactions.

corresponding scale for hadronization of a quark ($2C_F\mathcal{A} \simeq 0.5 \text{ GeV}$) or a gluon ($2C_A\mathcal{A} \simeq 1.0 \text{ GeV}$). In all cases the scale relates to the amount of radiation per unit rapidity with respect to the emitter. The much larger scale associated with UE is not unexpected: one can either interpret it in terms of multiple gluon-gluon interactions between the proton remnants, or alternatively in terms of an effective perturbative saturation scale, induced by small- x dynamics; both would lead to substantially higher values of the effective scale than expected for normal hadronization.

Though not surprising, the large value of Λ_{UE} does have implications for choices of R in jet finding. Arguments based on purely perturbative considerations (and on normal hadronization) suggest that $R = 1$ is an optimal value. The non-perturbative scale associated with the UE is so large, however, that for moderate p_t jets it can easily be comparable to the perturbative contributions, proportional to $\alpha_s p_t$. This, for example, is the explanation for the poor behaviour of the k_t algorithm in [44] with the ‘recommended’ $R = 1$ choice, while smaller R values, used more recently for the k_t algorithm in [45], lead to more reasonable UE corrections. In contrast, when examining very high p_t jets, since the UE should be p_t independent, it will become advantageous to return to $R \sim 1$, so as to minimise the size of perturbative corrections, which behave roughly as $\sim \alpha_s p_t \ln R$.

5. Experimental considerations

There are a number of respects in which the results presented above are relevant experimentally. On one hand, knowledge of the relative size of various non-perturbative and perturbative contributions as a function of R can provide guidance in the choice of optimal values of R . On the other hand, experimental data can provide interesting cross-checks of our understanding of the R dependence, for example through direct measurements of how the transverse momentum of a jet depends on the parameters of jet algorithm, and through studies of quantities such as inclusive jet cross sections. In what follows, we will sketch three possible avenues of experimental investigation on these issues; they should be seen as examples of what could be done, which will have to be adapted to the chosen observable and to the needs of the given experimental setup.

5.1 Radius optimisation

We have seen that there are three main sources of corrections to the transverse momentum of a jet: perturbative radiation; hadronization, *i.e.* non-perturbative effects associated with the jet itself; and the underlying event, *i.e.* low- p_t effects associated with proton-remnant interactions. Each of these effects has a different dependence on the jet p_t , on the colour factor associated with the hard parton originating the jet, on the choice of R in the jet finder, and finally on the collider energy, as illustrated in table 1.

Let us examine the implications of this understanding on the choice of R in various experimental contexts. There are two principal scenarios to be considered, corresponding to two rather different usages of jets. One may use jets for the identification of underlying kinematic structures, such as mass peaks for the top quark or other heavy particles, or in a search for hadronic decays of a hypothetical Z' . Alternatively, one may wish to compare jet

	Dependence of jet $\langle \delta p_t \rangle$ on			
	‘partonic’ p_t	colour factor	R	\sqrt{s}
perturbative radiation	$\sim \alpha_s(p_t) p_t$	C_i	$\ln R + \mathcal{O}(1)$	–
hadronization	–	C_i	$-1/R + \mathcal{O}(R)$	–
underlying event	–	–	$R^2 + \mathcal{O}(R^4)$	s^ω

Table 1: Summary of the main physical effects that contribute to the relation between the transverse momentum of a jet and that of a parton, together with their dependence on the properties of the parton, the jet radius R and collider centre of mass energy. Cases labelled “–” do not have any dependence on the corresponding variable in a leading approximation, but may develop anomalous-dimension type dependences at higher orders.

data (such as the inclusive jet spectrum) with high-order perturbative QCD calculations, and attempt to deduce information about fundamentals of QCD or the electroweak theory. In the first case, one seeks to extract the cleanest possible kinematic structures, and therefore one should minimise both perturbative and non-perturbative modifications of a jet p_t ; in the second case, one presumes that the perturbative loss is calculated with good precision for typical ranges of R , and one wishes to minimise the two non-perturbative contributions, since they cannot be precisely computed from first principles.

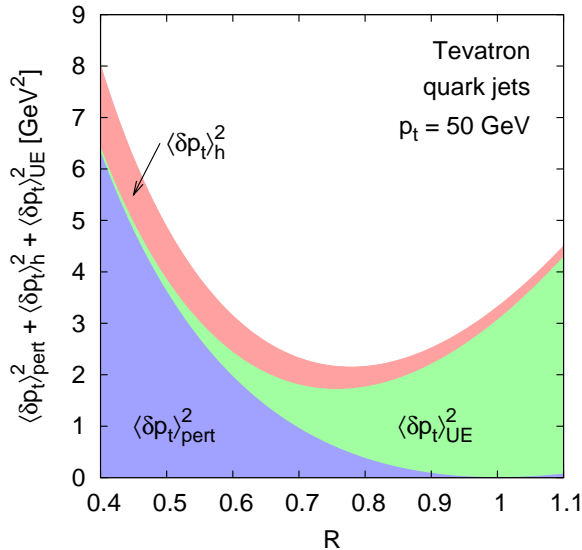


Figure 5: Contributions to the average δp_t^2 from perturbative radiation, hadronization and underlying event, for quark jets at the Tevatron, as a function of R . For the perturbative contribution we have used Eq. (2.7); for the hadronization contribution we have taken just the $1/R$ term; for UE we have used the full R dependence and set $\Lambda_{\text{UE}} = 4$ GeV.

When considering how well one can reconstruct kinematic structures such as mass peaks, one needs to know the dispersion due to both perturbative and non-perturbative effects, as well as any non-trivial correlations between them. Although this goes beyond the scope of what has been calculated in this paper, some basic quantitative information can nonetheless be obtained, by arguing that the dispersion on a jet p_t (and therefore on

any kinematic structure) can be approximated by the uncorrelated sum

$$\langle \delta p_t^2 \rangle \sim \langle \delta p_t \rangle_{\text{pert}}^2 + \langle \delta p_t \rangle_{\text{h}}^2 + \langle \delta p_t \rangle_{\text{UE}}^2. \quad (5.1)$$

This size of the summed squared contributions is shown as a function of R in Fig. 5, using our analytical results for the perturbative and for the two non-perturbative contributions, for 50 GeV quark jets, with the normalisation for the underlying event contribution set to $\Lambda_{\text{UE}} = 4$ GeV, corresponding roughly to `Pythia`'s estimate for the Tevatron. One observes that while perturbation theory prefers⁸ $R \simeq 1$, the significant underlying event contribution leads one to favour somewhat smaller values, $R \simeq 0.7 - 0.8$. For this p_t value, on the other hand, hadronization has a relatively limited effect.

One can make plots similar to Fig. 5 for a range of jet transverse momenta, for quark jets and gluons jets, and at Tevatron or at LHC. In each case one can determine an optimal R , minimising the combination of perturbative and non-perturbative contributions, Eq. (5.1). The results are shown, as a function of p_t , in Fig. 6.

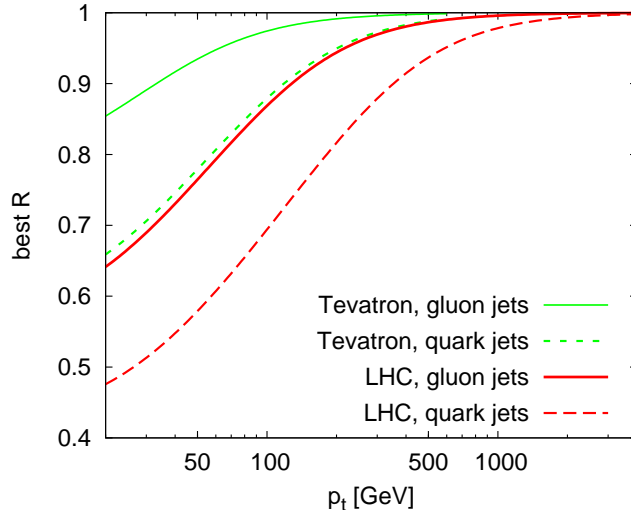


Figure 6: The R value that minimises the sum of squared average perturbative, hadronization and UE contributions, as a function of p_t . The approximations are the same as those in Fig. 5, except that for LHC we have used $\Lambda_{\text{UE}} = 10$ GeV.

One sees that in the high- p_t limit, where perturbative radiation dominates, R should be chosen $\simeq 1$, as expected, since this minimises $|\ln R|$. At lower transverse momentum, $p_t \sim 100$ GeV, the contribution from the UE, with its large intrinsic scale $\sim 4 - 10$ GeV becomes of similar relative importance as the perturbative $\alpha_s p_t$ term, so that it becomes advantageous to decrease R , in order to take advantage of the R^2 reduction of the UE contribution. As a consequence, even though on average jets are slightly narrower at high p_t than at low p_t (essentially because of the reduction of α_s), it is actually advantageous to

⁸The dispersion of the perturbative contribution will not of course precisely vanish for $R = 1$ — rather, Fig. 5 should be thought of as the extra dispersion over and above whatever minimal perturbative dispersion would be present for $R = 1$.

	quark jets	gluon jets
Tevatron	0.63	0.83
LHC	0.46	0.61

Table 2: R values that minimise the two non-perturbative contributions in various circumstances.

use *larger* R values at high p_t , because in absolute terms perturbative radiation is roughly proportional to p_t .

In contrast to this slightly counterintuitive result, when going from quark to gluon jets one’s intuition about the correlation between jet width and choice of R is reliable: for gluon jets, perturbative radiation and hadronization are both larger, whereas the underlying event is unchanged; the optimal R , therefore, is larger. One may finally note that at LHC one needs a smaller R than at Tevatron, because of the noisier underlying event.

The situation is different if one considers observables where perturbative effects are accounted for by higher-order calculations. One should then minimise just the sum of the squares of the hadronization and UE components. Ignoring all but the R^2 term of the UE contribution, this implies that the optimal R is given by

$$R = \sqrt{2} \left(\frac{C_i A(\mu_I)}{\Lambda_{\text{UE}}} \right)^{1/3}, \quad (5.2)$$

where, as usual, C_i is the colour factor for the hard parton responsible for the jet. Using the same values for Λ_{UE} as in Fig. 6, this gives the results in Table 2, which are independent of p_t to a first approximation, and actually correspond to the zero- p_t limit of Fig. 6.

It should be kept in mind that these results involve many approximations: for example, we have ignored differences between jet algorithms, we have used just the small R limit for some terms, we have assumed that average shifts are indicative of dispersions, and we have neglected the issue of actually being able to resolve separate jets for complex massive particle decays. We believe, nevertheless, that the basic conclusions are valid all the same: in reconstructing kinematic structures one should prefer larger R at high p_t and for gluon jets, and smaller R at the LHC than at the Tevatron; when perturbative effects are calculated separately, on the other hand, the minimisation of the non-perturbative contributions alone leads one to favour somewhat lower values of R .

5.2 Measurement of $\langle \delta p_t \rangle$

Throughout this article we have discussed the change in a jet transverse momentum due to perturbative and non-perturbative effects. It should be emphasised, however, that this $\langle \delta p_t \rangle$ is not an operationally well-defined quantity away from the threshold limit. The reason is that we have imagined using a parton to provide a reference transverse momentum, with respect to which we then discuss the shift $\langle \delta p_t \rangle$. Beyond leading order, collinear divergences and quantum mechanical interference between emissions make the choice of a reference parton p_t inherently ambiguous. Were we discussing e^+e^- collisions, this would not be a serious issue, since the e^+e^- centre of mass energy itself would provide a meaningful reference scale. At hadron colliders, however, and notably in dijet production, such an unambiguous reference scale seldom exists.

To study directly the shift $\langle \delta p_t \rangle$, either at NLO or experimentally, one must therefore find a physical way of identifying a reference scale for the jet. One possible approach, which we propose to follow here, is to introduce a reference jet definition, D_{ref} , and then measure how a jet transverse momentum changes if one uses an alternative definition D_{alt} . One complication is that different jet definitions lead, in principle, to different sets of jets, so that one must be able to identify which jet, with definition D_{alt} , corresponds to a given jet with definition D_{ref} . An algorithm for doing so could be outlined as follows.

1. Identify the set of reference jets that are of interest, $j_{\text{ref}}^{(1)}, \dots, j_{\text{ref}}^{(n)}$, for example the two hardest jets in the event, using the definition D_{ref} .
2. Associate with each jet in the reference set, $j_{\text{ref}}^{(i)}$, the alternate jet $j_{\text{alt}}^{(k)}$ with which it shares the most p_t . In other words, find the k that maximises

$$p_t^{(ki)} = \sum_{\ell \in j_{\text{alt}}^{(k)} \cap j_{\text{ref}}^{(i)}} p_{t,\ell} , \quad (5.3)$$

where the sum runs over particles ℓ that are contained in both jets.

3. Reject events in which the same alternate jet is associated with multiple reference jets⁹, as well as events in which a reference jet $j_{\text{ref}}^{(i)}$ shares no p_t with any of the $j_{\text{ref}}^{(k)}$, $p_t^{(ki)} = 0, \forall k$.
4. Discard alternate jets that have not been associated with any reference jets.

Being interested, say, in the R dependence of $\langle \delta p_t \rangle$, one might then perform the following analysis. Begin by selecting, with the reference algorithm, events in which the two hardest jets are both central, so that they are well measured (set, for example, $|y_{\text{ref}}^{(i)}| < 2$); require the sum of the jet p_t 's to be in a some limited range, for example $55 \text{ GeV} < \frac{1}{2}(p_{t,\text{ref}}^{(1)} + p_{t,\text{ref}}^{(2)}) < 70 \text{ GeV}$; repeat the jet finding with the same jet algorithm but with an alternate radius R_{alt} ; find the jets that match the two reference jets, and determine the difference in p_t between the alternate and reference jet definitions, using

$$\delta p_t = \frac{1}{2} \left(p_{t,\text{alt}}^{(1)} + p_{t,\text{alt}}^{(2)} - p_{t,\text{ref}}^{(1)} - p_{t,\text{ref}}^{(2)} \right) . \quad (5.4)$$

For illustrative purposes, this procedure has been carried out on LHC events simulated with `Pythia` and with `Herwig`, and the resulting $\langle \delta p_t \rangle$ is shown Fig. 7, both at parton level and at hadron level (including hadronization and UE). We used the Cambridge/Aachen algorithm with reference jet radius $R_{\text{ref}} = 0.7$. One notes that the moderate differences between the `Pythia` tune A and `Jimmy` underlying events (cf. Fig. 3) are clearly visible here. One also observes that perturbative and non-perturbative effects are of comparable sizes.

⁹In the studies described below, we find that this occurs only very rarely: in a fraction of a percent of events when using the Cambridge/Aachen algorithm both as reference and alternate, and in a couple of percent of events if the alternate algorithm is `SISCone`.

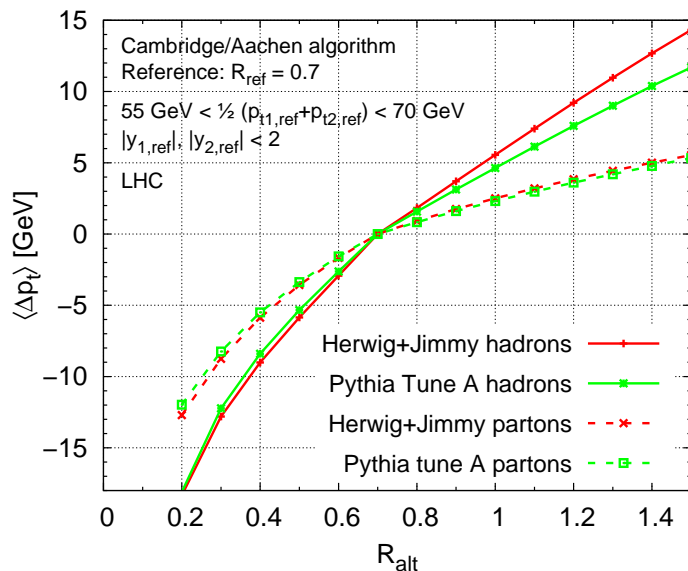


Figure 7: The average shift, $\langle \delta p_t \rangle$, as defined in Eq. (5.4), between an alternate (Cambridge/Aachen with variable R_{alt}) and a reference jet definition (the same algorithm, with fixed $R_{\text{ref}} = 0.7$), determined from Monte Carlo simulation. Hadron level results include the UE contribution, whereas at parton level it has been switched off. See text for further details.

Given a measurement of $\langle \delta p_t \rangle$, an interesting study would be to compute the average p_t change at NLO, $\langle \delta p_t \rangle_{\text{NLO}}$, for example with `NLOjet++` [46]. Such a calculation would include configurations with up to three partons in a jet (a level of detailed jet structure that is reached in the inclusive jet spectrum only at NNLO). Given this accurate perturbative knowledge of δp_t , one could then fit the two non-perturbative components, in order to get data-based constraints on their magnitude independent of parton shower Monte Carlos. Specifically, one would write¹⁰

$$\begin{aligned} \langle \delta p_t \rangle(R_{\text{alt}}) = & \langle \delta p_t \rangle_{\text{NLO}}(R_{\text{alt}}) - 2 \langle C_i \rangle \left(\frac{1}{R_{\text{alt}}} - \frac{1}{R_{\text{ref}}} \right) \mathcal{A}(\mu_I) \\ & + (R_{\text{alt}} J_1(R_{\text{alt}}) - R_{\text{ref}} J_1(R_{\text{ref}})) \Lambda_{\text{UE}}, \end{aligned} \quad (5.5)$$

where $\langle C_i \rangle$ is the average colour factor that takes into account the fraction of quark and gluon jets. Using Eq. (5.5), one would be able to fit the two non-perturbative parameters $\mathcal{A}(\mu_I)$ and Λ_{UE} . One would expect $\mathcal{A}(\mu_I)$ to agree qualitatively with value extracted from event shape studies in e^+e^- annihilation and DIS [13], and one would obtain a first direct estimate of Λ_{UE} .

A similar analysis could also be carried out in other contexts, for example W +jet events. In that case one would consider only a single reference jet, and one could use `MCFM` [47, 48] for the perturbative calculation. Since the fraction of quark and gluon jets would be rather different in this case, compared to inclusive jets (especially at LHC), this would provide a powerful check of the dependence of hadronization on partonic colour

¹⁰The hadronization terms of higher order in R have been neglected here, since in the region of R where they contribute significantly they are dominated by the UE contribution.

factors, and it would also test whether the UE is independent of the underlying hard partonic reaction, as expected in many simple models.

5.3 Inclusive jet spectrum

A context where non-perturbative corrections to jets have often been discussed [17, 18] is the inclusive jet p_t spectrum. In Ref. [17], for example, one sees that introducing a non-perturbative shift in p_t is necessary in order to fit data for the ratio of inclusive distributions measured at UA1 and at Tevatron. In order to estimate the effects of the nonperturbative shift we have computed here, let us begin by assuming that we have at our disposal a jet definition such that quark and gluon jets can be distinguished at parton level (an example of such a definition is given in [49]), and such that it can be consistently employed at hadron level as well (which is not the case for the definition in [49]). Then we would be able to write

$$\frac{d\sigma}{dp_t}(p_t) = \frac{d\sigma^{q,\text{PT}}}{dp_t}(p_t - \langle\delta p_t^q\rangle_{\text{NP}}) + \frac{d\sigma^{g,\text{PT}}}{dp_t}(p_t - \langle\delta p_t^g\rangle_{\text{NP}}), \quad (5.6)$$

where $d\sigma^{i,\text{PT}}/dp_t$ is the perturbative distribution for jets of flavor i , which is then evaluated with an i -dependent shift

$$\langle\delta p_t^i\rangle_{\text{NP}} = -2 \frac{C_i}{R} \mathcal{A}(\mu_I) + R J_1(R) \Lambda_{\text{UE}}. \quad (5.7)$$

It should be emphasised that, even at this stage, Eq. (5.6) relies on several approximations: it assumes, for example, that one can neglect the effect of event-by-event fluctuations in the hadronization and UE contributions, and it assumes that non-perturbative effects are dominated by an overall shift in the distribution. This is essentially the same approximation that led to the broadly successful use of a constant shift in place of a shape function when studying non-perturbative effects in event-shape distributions (as in [7, 50, 51], see however also [52–55]). One should note that here, even at the level of single gluon exchange, soft gluon resummation near threshold suggests that the distribution will be distorted, and not simply shifted, due to colour mixing effects [15]. It can be shown, however, that the leading $1/R$ term is not affected by colour mixing in the context of NLL resummation. We can then safely assume that the shift in Eq. (5.7) is the dominant effect: the first term is large for $R < 1$, while the second term is large because of the large value of Λ_{UE} .

In practice, Eq. (5.6) is inconvenient because of our inability to separately define $\sigma^{q,\text{PT}}$ and $\sigma^{g,\text{PT}}$ beyond leading order (LO), for jet algorithms that are valid also at hadron level. We may however further simplify Eq. (5.6) by expanding in the small relative shifts $\langle\delta p_t^i\rangle_{\text{NP}}/p_t$. To this end, let us define

$$n_i \equiv -\frac{d \ln (d\sigma^{i,\text{PT}}/dp_t)}{d \ln p_t}, \quad f_i \equiv \frac{d\sigma^{i,\text{PT}}}{dp_t} \bigg/ \frac{d\sigma^{\text{PT}}}{dp_t}, \quad (5.8)$$

which represent respectively the power-law fall-off of the distribution, which behaves as $p_t^{-n_i}$, and the fraction of jets that are of species i . We can then write

$$\frac{d\sigma}{dp_t}(p_t) = \frac{d\sigma^{q,\text{PT}}}{dp_t}(p_t) \left(1 + n_q \frac{\langle\delta p_t^q\rangle_{\text{NP}}}{p_t} + \mathcal{O}\left(n_q^2 \frac{\langle\delta p_t^q\rangle_{\text{NP}}^2}{p_t^2}\right) \right) + (q \leftrightarrow g), \quad (5.9)$$

We note that the neglected term in Eq. (5.9) is expected to be of the same magnitude as terms that would arise from the replacement of the shift with a shape function. Finally we rewrite Eq. (5.9) as

$$\frac{d\sigma}{dp_t}(p_t) = \frac{d\sigma^{\text{PT}}}{dp_t} \left(p_t - \frac{f_q n_q \langle \delta p_t^q \rangle_{\text{NP}} + f_g n_g \langle \delta p_t^g \rangle_{\text{NP}}}{f_q n_q + f_g n_g} + \mathcal{O} \left(n_i^2 \frac{\langle \delta p_t^i \rangle_{\text{NP}}^2}{p_t} \right) \right). \quad (5.10)$$

In Eq. (5.10), one can evaluate $d\sigma^{\text{PT}}/dp_t$ up to NLO (or beyond) since it is summed over jet flavors, while for the purpose of calculating the (small) non-perturbative shift, f_i and n_i can be evaluated at LO, where the jet flavour is unambiguous. Generalising Eq. (5.10) to include not only $1/R$ hadronization terms, but also subleading powers of R , is a nontrivial task: one would have to sum not over q and g jets, but rather over all different scattering channels ($qq \rightarrow qq$, $qg \rightarrow qg$, $gg \rightarrow gg$, etc.), and furthermore the threshold approximation suggests that colour correlations would make it necessary to go beyond the shift approximation. These subleading terms would therefore be quite interesting from a theoretical viewpoint, while they are unlikely to have a significant phenomenological impact, given the likely experimental constraints in the difficult environment of hadron-hadron collisions. For phenomenological applications, on the other hand, a further and final approximation can be made on Eq. (5.10), if one assumes that quark and gluon species have a similar power-law fall-off, $n_q \simeq n_g$. One can then simply write

$$\frac{d\sigma}{dp_t}(p_t) \simeq \frac{d\sigma^{\text{PT}}}{dp_t} \left(p_t - \langle \delta p_t \rangle_{\text{NP}} \right), \quad \langle \delta p_t^{\text{NP}} \rangle = f_q \langle \delta p_t^q \rangle_{\text{NP}} + f_g \langle \delta p_t^g \rangle_{\text{NP}}, \quad (5.11)$$

Again, this can be extended, if one wishes, to separately consider all $2 \rightarrow 2$ scattering channels, however a full treatment of the $\mathcal{O}(R)$ terms in the hadronization correction will probably require that the prediction be rephrased in the language of shape functions.

To conclude, we observe that in addition to the inclusive jet spectrum directly, one may also examine the relative difference between the distributions that emerge when using two different jet definitions, in analogy to what was done in Section 5.2. One may define

$$\rho(D_{\text{ref}}, D_{\text{alt}}, p_t) = \left(\frac{d\sigma^{\text{alt}}}{dp_t} - \frac{d\sigma^{\text{ref}}}{dp_t} \right) / \left(\frac{d\sigma^{\text{ref}}}{dp_t} \right). \quad (5.12)$$

Perturbatively, with current tools [46], the numerator can be studied up to α_s^4 , because the α_s^2 term vanishes; in other words, this is effectively a three-jet observable, which can be calculated to NLO, and thus this is a quantity that can be studied to higher perturbative order than the inclusive jet spectrum itself (for which α_s^4 would correspond to NNLO). Eq. (5.12) is similar in this respect to the difference in p_t between alternate and reference definitions discussed in Section 5.2. The separation of ρ into perturbative and non-perturbative parts reads

$$\begin{aligned} \rho(D_{\text{ref}}, D_{\text{alt}}, p_t) &= \rho^{\text{PT}}(D_{\text{ref}}, D_{\text{alt}}, p_t) \\ &+ \frac{1}{p_t} \left[f_q n_q \left(\langle \delta p_t^q \rangle_{\text{NP,alt}} - \langle \delta p_t^q \rangle_{\text{NP,ref}} \right) + f_g n_g \left(\langle \delta p_t^g \rangle_{\text{NP,alt}} - \langle \delta p_t^g \rangle_{\text{NP,ref}} \right) \right]. \end{aligned} \quad (5.13)$$

Clearly, these techniques can also be applied to ratios of distributions measured with different centre-of-mass energies (as in [17]), or differing with respect to other parameters. In

this way one may attempt to minimise or isolate the perturbative contribution, and get a better handle on our non-perturbative inputs. When these are established, one may apply the resulting shift to the distribution itself, in order to optimise the analysis in view of other QCD or new physics studies.

6. Conclusions

We have performed a first broad analysis of non-perturbative QCD effects on jet observables at hadron colliders such as Tevatron or the LHC, examining hadronization effects and underlying event corrections, and studying how they compare to perturbative contributions. We have used both analytic models, within the framework of the dispersive approach, and different Monte Carlo tools, implementing different IRC-safe jet algorithms, belonging to both the ‘cone’ and ‘sequential recombination’ families of jet finders. Finally, we have considered different observables, focusing mostly on the shift in the transverse momentum of a jet due to QCD radiation, but giving results also for the jet mass and for the jet p_t distribution.

Our most significant results are displayed in Eq. (4.1) and Eq. (4.2), and collected in Table 1. They show that the transverse momentum of a jet of radius R is modified by hadronization effects in a manner proportional to $1/R$, while underlying event corrections grow like R^2 , increasing with the jet area. A similar pattern holds for our analysis of the jet mass, where in general the correction is suppressed by two powers of R with respect to the p_t analysis, but with the same hierarchy between hadronization and underlying event. As we briefly reviewed, the perturbative R -dependence for the jet p_t is logarithmic at small R . We thus have three different functional forms for the R -dependence of the three main contributions to the jet momentum. This leads to the possibility of selectively minimising chosen combinations of these three effects, by a suitable choice of R , in order to optimise a given physics analysis.

Our results are formulated in terms of two different non-perturbative parameters: the first, $\mathcal{A}(\mu_I)$, describes hadronization, and we expect it to be closely related to similar parameters measured in event-shape studies in e^+e^- annihilation, a conjecture which is consistent with the Monte Carlo results; the second parameter, Λ_{UE} , describes the flow of transverse momentum per unit rapidity due to underlying hadronic activity in a given collider environment: its value must be extracted from data and is expected to be universal across different observables in a given collider, while it should scale with a power of the centre-of-mass energy. A further characterisation is provided by the dependence of transverse momentum on the colour charge of the parton originating the jet: in our approximations, both perturbative and hadronization contributions are proportional to the colour charge, while the underlying event is independent of it.¹¹

These results are rather strikingly confirmed by our studies with Monte Carlo simulations. Hadronization corrections, as given by non-perturbative models embedded in `Herwig` and `Pythia`, indeed grow at small R , broadly agreeing with the analytic estimate both in

¹¹Work is already in progress [42] to understand how perturbative and UE effects interact, so as to introduce a subleading dependence on the jet colour factor in the UE contribution.

shape and normalisation, while the corresponding underlying event corrections (computed with Jimmy for the Herwig simulation) grow with R as expected.

Finally, we have given three examples of experimental studies where our results could be either tested or used in order to perform physics analyses. Specifically, we have outlined how our results are likely to impact the single-inclusive jet p_t distribution, a signature observable at hadron colliders in general and at LHC in particular; we have indicated how the p_t shift from parton to hadron level could be experimentally accessed in order to test our calculation; and we have suggested methods and choices in order to optimise the value of the jet radius in view of different experimental situations.

We regard these suggestions as just basic examples of the studies that could be performed. More generally, we believe that our study emphasises the necessity for variety and flexibility in the experimental choices of jet definitions and parameters. In the early days of QCD, when theoretical predictions were mostly at leading order in perturbation theory, it was reasonable to adopt a rough definition of a jet, and several such definitions proved sufficient to gather striking evidence for many basic features of QCD and of the standard model. Those days are past: QCD is now precision physics, with NLO calculations forming the standard benchmark for predictions, selected observables having been computed at higher orders, and all-order resummations and power correction studies also available. From an experimental point of view, the challenges of the high-luminosity, high-energy environment of the LHC will require that all the experience acquired with previous accelerators, and all our theoretical knowledge, be put to good use.

We believe that in order to do that it will be necessary to take advantage of the full flexibility offered by modern jet tools. There are now several well-tested IRC-safe jet algorithms, both of cone type and based on sequential recombination. They depend on parameters, notably the radius R , which provide the experimenter with handles to control the flow and impact of perturbative and non-perturbative QCD radiation. Exploiting the adaptability of these jet tools will be crucial for model testing, for the validation of experimental procedures, and, last but not least, for studies that will further our understanding of the strong interactions.

Acknowledgements

We thank Matteo Cacciari for collaboration in the initial stages of this project and Jon Butterworth, Arthur Moraes, Torbjorn Sjöstrand and Peter Skands for discussions. We are grateful to each other's home institution, as well as to the Galileo Galilei Institute (Florence, Italy), and to the CERN Theory Division for hospitality during the completion of this work. MD thanks the CNRS for a visiting fellowship during the period in which this collaboration was initiated. Work supported by MIUR under contract 2006020509_004, by the French ANR under contract ANR-05-JCJC-0046-01 and by the European Community's Marie-Curie Research Training Network 'Tools and Precision Calculations for Physics Discoveries at Colliders' ('HEPTOOLS'), under contract MRTN-CT-2006-035505.

Appendix

Here we compute the global term involving the integral of the unrecombined gluon contribution δp_t^- , defined in Eq. (3.9), over all of phase space, to show that after accounting for the evolution of parton distributions it does not contribute any linear power correction. To illustrate the point, we consider the dipole formed by the two incoming legs, discussed in Section 3.3. To restrict our attention to soft emission alone we impose a cutoff, requiring that the longitudinal fraction (with respect to the beam) of the emitted gluon momentum k never exceed ϵ_c , implying $|\eta| < \eta_{\max}(k_t) = \ln \epsilon_c \sqrt{s}/k_t$. The relevant integral is then

$$\langle \delta p_t \rangle_{\text{gl}}^{(12)} = -\frac{C_F}{\pi} \int dk_t \delta\alpha_s(k_t) d\eta \frac{d\phi}{2\pi} (\cosh(\eta) + \cos\phi). \quad (1)$$

Here we have set the colour factor of the dipole C_{12} to be $2C_F$, since we are interested only in the radiation collinear to the incoming legs, which we take to be quarks. In actual fact the colour charge C_F for each leg will be built up from a sum of dipole contributions, all of which involve the incoming leg in question and give the same result in the collinear limit: the replacement of the dipole colour factor by $2C_F$ anticipates this fact. To illustrate our point, but without loss of generality, we use a toy model for the non-perturbative coupling, setting $\delta\alpha_s(k_t) = \Lambda\delta(k_t - \Lambda)$. In this model the quantity \mathcal{A} , which governs our leading power corrections computed in Section 3, is just proportional to Λ . After performing the integral over the full range of azimuth ϕ , the global term gives

$$\begin{aligned} \langle \delta p_t \rangle_{\text{gl}}^{(12)} &= -\frac{C_F}{\pi} \int \delta\alpha_s(k_t) dk_t \int_{-\eta_{\max}}^{\eta_{\max}} d\eta \cosh\eta \\ &= -\frac{2C_F}{\pi} \int \delta\alpha_s(k_t) dk_t \sinh\eta_{\max} \\ &= -\frac{C_F}{\pi} \cdot \epsilon_c \sqrt{s} + \mathcal{O}\left(\frac{\Lambda^2}{\sqrt{s}}\right). \end{aligned} \quad (2)$$

As we shall see, the dependence on the cutoff ϵ_c will be removed by a similar term due to the evolution of the parton distributions. Note then the absence of any term of order Λ , and hence the absence of a leading power correction due to this global term.

In order to verify the factorisability of the collinear divergence in Eq. (2), let us now turn to the contribution of parton distributions. In the calculations presented in section 3 we worked in the threshold limit, effectively approximating parton distributions with their bare expression at threshold, $q_0(x) = \delta(1-x)$. In our non-perturbative approximation, the distribution evolved to a hard scale Q is then given by

$$\begin{aligned} q(x, Q^2) &= \delta(1-x) + \frac{2C_F}{\pi} \int_{1-\epsilon_c}^1 \frac{dz}{1-z} \int_{Q_0}^Q \frac{dk_t}{k_t} \delta\alpha_s(k_t) (\delta(x-z) - \delta(1-x)), \\ &= \delta(1-x) + \frac{2C_F}{\pi} \int_{1-\epsilon_c}^1 \frac{dz}{1-z} (\delta(x-z) - \delta(1-x)), \end{aligned} \quad (3)$$

where Q_0 is an arbitrary reference scale, we have placed the same cutoff as in Eq. (2) on the maximum emitted longitudinal momentum, and we have used the infrared limit ($z \rightarrow 1$)

of the quark splitting function $P_{qq}(z)$. Note that when one considers parton evolution one automatically includes collinear branchings which push the hard scattering away from threshold.

Taking into account parton evolution, we are then forced to include a further non-perturbative shift in the transverse momentum of the jet, given by

$$\begin{aligned}
\langle \delta p_t \rangle_{\text{PDF}} &= \int dx_1 dx_2 \frac{\sqrt{x_1 x_2 s}}{2} (q(x_1, Q^2) q(x_2, Q^2) - q_0(x_1) q_0(x_2)) \\
&= \frac{2C_F}{\pi} \left(\int_{1-\epsilon_c}^1 \frac{dz_1}{1-z_1} \frac{(\sqrt{z_1}-1)\sqrt{s}}{2} + (1 \leftrightarrow 2) \right) \\
&= -\frac{C_F}{\pi} \epsilon_c \sqrt{s} + \mathcal{O}(\epsilon_c^2).
\end{aligned} \tag{4}$$

One observes that the collinear divergence in Eq. (2) has precisely the form required to be absorbed in a ‘renormalised’ parton distribution, such as the one computed in Eq. (4). Eq. (2) then assures us that the remaining finite terms do not contain leading power corrections.

Similar calculations can be carried out for all dipoles, and in each case one observes that no $\mathcal{O}(\Lambda)$ term arises from ‘global’ integrations over all phase space. For each dipole, furthermore, collinear divergences can either be factorised into the parton distribution, as done above, or they cancel, as in the case of outgoing legs, against an identical divergence in the ‘in-jet’ contribution, as expected from the collinear safety of our observables.

References

- [1] N. Kidonakis and G. Sterman, Nucl. Phys. B **505** (1997) 321, [hep-ph/9705234](#).
- [2] N. Kidonakis, G. Oderda and G. Sterman, Nucl. Phys. B **525** (1998) 299, [hep-ph/9801268](#).
- [3] N. Kidonakis, G. Oderda and G. Sterman, Nucl. Phys. B **531** (1998) 365, [hep-ph/9803241](#).
- [4] N. Kidonakis and J. F. Owens, Phys. Rev. D **63** (2001) 054019, [hep-ph/0007268](#).
- [5] D. de Florian and W. Vogelsang, Phys. Rev. D **76** (2007) 074031, [arXiv:0704.1677 \[hep-ph\]](#).
- [6] M. H. Seymour, Nucl. Phys. B **513** (1998) 269, [hep-ph/9707338](#).
- [7] G. P. Korchemsky and G. Sterman, Nucl. Phys. B **437** (1995) 415, [hep-ph/9411211](#).
- [8] Y. L. Dokshitzer and B. R. Webber, Phys. Lett. B **352** (1995) 451, [hep-ph/9504219](#).
- [9] P. Ball, M. Beneke and V. M. Braun, Nucl. Phys. B **452** (1995) 563, [hep-ph/9502300](#).
- [10] Y. L. Dokshitzer, G. Marchesini and B. R. Webber, Nucl. Phys. B **469** (1996) 93, [hep-ph/9512336](#).
- [11] E. Gardi, Nucl. Phys. B **622** (2002) 365, [hep-ph/0108222](#).
- [12] M. Beneke, Phys. Rept. **317** (1999) 1, [hep-ph/9807443](#).
- [13] M. Dasgupta and G. P. Salam, J. Phys. G **30** (2004) R143, [hep-ph/0312283](#).
- [14] A. Banfi, G. Marchesini, G. Smye and G. Zanderighi, JHEP **0108**, 047 (2001), [hep-ph/0106278](#).

- [15] M. Dasgupta and Y. Delenda, [arXiv:0709.3309 \[hep-ph\]](#).
- [16] A. Bhatti *et al.*, Nucl. Instrum. Meth. **A 566** 375 (2006), [hep-ex/0510047](#).
- [17] M. L. Mangano, [hep-ph/9911256](#).
- [18] J. M. Campbell, J. W. Huston and W. J. Stirling, Rept. Prog. Phys. **70** (2007) 89, [hep-ph/0611148](#).
- [19] S. D. Ellis, J. Huston, K. Hatakeyama, P. Loch and M. Toennesmann, [arXiv:0712.2447 \[hep-ph\]](#).
- [20] T. Sjostrand, S. Mrenna and P. Skands, JHEP **0605** (2006) 026, [hep-ph/0603175](#).
- [21] G. Corcella *et al.*, [hep-ph/0210213](#).
- [22] J. M. Butterworth, J. R. Forshaw and M. H. Seymour, Z. Phys. C **72** (1996) 637, [hep-ph/9601371](#).
- [23] C. Lee and G. Sterman, Phys. Rev. D **75** (2007) 014022, [hep-ph/0611061](#).
- [24] M. Furman, Nucl. Phys. B **197** (1982) 413.
- [25] F. Aversa, P. Chiappetta, M. Greco and J. P. Guillet, Nucl. Phys. B **327** (1989) 105; Z. Phys. C **46** (1990) 253.
- [26] J. P. Guillet, Z. Phys. C **51** (1991) 587.
- [27] B. Jager, M. Stratmann and W. Vogelsang, Phys. Rev. D **70** (2004) 034010, [hep-ph/0404057](#).
- [28] S. Catani, Y. L. Dokshitzer, M. H. Seymour and B. R. Webber, Nucl. Phys. B **406** (1993) 187 and refs. therein.
- [29] S. D. Ellis and D. E. Soper, Phys. Rev. D **48** (1993) 3160, [hep-ph/9305266](#).
- [30] Y. L. Dokshitzer, G. D. Leder, S. Moretti and B. R. Webber, JHEP **9708**, 001 (1997), [hep-ph/9707323](#); M. Wobisch and T. Wengler, [hep-ph/9907280](#).
- [31] G. P. Salam and G. Soyez, JHEP **0705** (2007) 086, [arXiv:0704.0292 \[hep-ph\]](#).
- [32] G. C. Blazey *et al.*, [hep-ex/0005012](#).
- [33] S. Catani, B. R. Webber and G. Marchesini, Nucl. Phys. B **349** (1991) 635.
- [34] R. K. Ellis, W. J. Stirling and B. R. Webber, Camb. Monogr. Part. Phys. Nucl. Phys. Cosmol. **8** (1996) 1.
- [35] Y. L. Dokshitzer, A. Lucenti, G. Marchesini and G. P. Salam, Nucl. Phys. B **511** (1998) 396 [Erratum-ibid. B **593** (2001) 729], [hep-ph/9707532](#).
- [36] Y. L. Dokshitzer, A. Lucenti, G. Marchesini and G. P. Salam, JHEP **9805** (1998) 003, [hep-ph/9802381](#).
- [37] M. Dasgupta and B. R. Webber, JHEP **9810** (1998) 001, [hep-ph/9809247](#).
- [38] M. Dasgupta, L. Magnea and G. Smye, JHEP **9911** (1999) 025, [hep-ph/9911316](#).
- [39] G. E. Smye, JHEP **0105** (2001) 005, [hep-ph/0101323](#).
- [40] M. Cacciari, G. P. Salam and G. Soyez, LPTHE-07-03, in preparation.
- [41] M. Cacciari and G. P. Salam, [arXiv:0707.1378 \[hep-ph\]](#).
- [42] M. Cacciari, G. P. Salam and G. Soyez, LPTHE-07-02, in preparation.

- [43] M. G. Albrow *et al.* [TeV4LHC QCD Working Group], [hep-ph/0610012](#).
- [44] V. M. Abazov *et al.* [D0 Collaboration], *Phys. Rev. D* **65** (2002) 052008, [hep-ex/0108054](#).
- [45] A. Abulencia *et al.* [CDF - Run II Collaboration], *Phys. Rev. D* **75** (2007) 092006 [Erratum-*ibid.* *D* **75** (2007) 119901], [hep-ex/0701051](#); A. Abulencia *et al.* [CDF II Collaboration], *Phys. Rev. Lett.* **96** (2006) 122001, [hep-ex/0512062](#).
- [46] Z. Nagy, *Phys. Rev. D* **68** (2003) 094002, [hep-ph/0307268](#).
- [47] J. Campbell and R. K. Ellis, *Phys. Rev. D* **65** (2002) 113007, [hep-ph/0202176](#).
- [48] J. Campbell, R. K. Ellis and D. L. Rainwater, *Phys. Rev. D* **68** (2003) 094021, [hep-ph/0308195](#).
- [49] A. Banfi, G. P. Salam and G. Zanderighi, *Eur. Phys. J. C* **47** (2006) 113, [hep-ph/0601139](#).
- [50] Y. L. Dokshitzer and B. R. Webber, *Phys. Lett. B* **404** (1997) 321, [hep-ph/9704298](#).
- [51] E. Gardi and J. Rathsman, *Nucl. Phys. B* **609** (2001) 123, [hep-ph/0103217](#).
- [52] E. Gardi and J. Rathsman, *Nucl. Phys. B* **638** (2002) 243, [hep-ph/0201019](#).
- [53] E. Gardi and L. Magnea, *JHEP* **0308** (2003) 030, [hep-ph/0306094](#).
- [54] C. F. Berger and G. Sterman, *JHEP* **0309** (2003) 058, [hep-ph/0307394](#).
- [55] C. F. Berger and L. Magnea, *Phys. Rev. D* **70** (2004) 094010, [hep-ph/0407024](#).